Environmental Toxicology and Chemistry

Critical Review

INTERACTIONS OF METAL-BASED ENGINEERED NANOPARTICLES WITH AQUATIC HIGHER PLANTS: A REVIEW OF THE STATE OF CURRENT KNOWLEDGE

MELUSI THWALA, STEPHEN J. KLAINE, and NDEKE MUSEE

Environ Toxicol Chem., **Accepted Article** • DOI: 10.1002/etc.3364

Critical Review **Environmental Toxicology and Chemistry**
DOI 10.1002/etc.3364

INTERACTIONS OF METAL-BASED ENGINEERED NANOPARTICLES WITH AQUATIC HIGHER PLANTS: A REVIEW OF THE STATE OF CURRENT KNOWLEDGE

Running title: Engineered nanoparticles interactions with aquatic plants

MELUSI THWALA, †‡ STEPHEN J. KLAINE, §‖ and NDEKE MUSEE*#

†Source Directed Scientific Measures Research Group, Council for Scientific and Industrial Research, Pretoria, South Africa

‡Zoology Department, University of Johannesburg, Johannesburg, South Africa

§Department of Biological Sciences, Clemson, South Carolina, USA

‖School of Biological Sciences, North-West University, Potchefstroom, South Africa

#Department of Chemical Engineering, University of Pretoria, Pretoria, South Africa

* Address correspondence to ndeke.musee@up.ac.za

Submitted 11 September 2015; Returned for Revision 14 December 2015; Accepted 7 January 2016

Abstract: The rising potential for the release of engineered nanoparticles (ENPs) into aquatic environments requires evaluation of risks in order to protect ecological health. The present review examined knowledge pertaining the interactions of metal-based ENPs with aquatic higher plants, identified information gaps and raised considerations for future research to advance knowledge on the subject. The discussion focused on ENPs' (i) bioaccessibility; (ii) uptake, adsorption, translocation and bioaccumulation, and (iii) their toxicity effects on aquatic higher plants. An information deficit surrounds the uptake of ENPs and associated dynamics because the influence of ENP characteristics and water quality conditions has not been well documented. Dissolution appears to be a key mechanism driving bioaccumulation of ENPs, whereas nanoparticulates often adsorb to plant surfaces with minimal internalisation. However, few reports document the internalisation of ENPs by plants, thus the role of nanoparticulates' internalisation in bioaccumulation and toxicity remain unclear, requiring further investigation. The toxicities of metal-based ENPs have mainly been associated with dissolution as a predominant mechanism, although *nano* toxicity has also been reported. To advance knowledge in this domain, future investigations need to integrate the influence of ENPs' characteristics and water physico-chemical parameters, as their interplay determines ENPs' bioaccessibility and influences their risk to health of aquatic higher plants. Furthermore, harmonisation of test protocols is recommended for fast tracking the generation of comparable data.

Keywords: Engineered nanoparticles, Aquatic plants, Bioaccessibility, Bioaccumulation, Nanoecotoxicology

INTRODUCTION

Concerns about the environmental health and safety of engineered nanomaterials (ENMs) emerged in the early 2000s as a result of uncertainties surrounding interactions with organisms, and reports of enhanced toxicity potential at nano scale [1,2,3,4]. For instance, as a result of nano scale dimensions, ENMs exhibit special physicochemical properties such as large surface area to mass ratio, high surface energy and reactivity [5,6], which distinguish them from bulk scale counterparts. Classes of ENMs are diverse and include carbon-based, quantum dots, metal and metal oxide nanoparticles. The focus of this review is specific to metal-based engineered nanoparticles (ENPs). Herein the term 'metal-based ENPs' collectively refers to both metals and metal oxide counterparts. This category of ENPs is the exclusive focus of this review because of their distinctive characteristics such as magnetism, catalytic capacity, and optoelectronic properties. Another important property is dissolution potential, i.e. the potential to release soluble metal species as free ions or metal complexes. The useful properties of metal-based ENPs mean that they are widely produced and incorporated into consumer products and industrial applications [7,8], and they are consequently increasingly being released into man-made [9,10,11] and natural aquatic systems [12].

The unique nano scale properties of ENPs mean that their environmental fate, behaviour, and toxicity may differ from those of bulk scale pollutants [13] such that traditional hazard and risk assessment models are no longer adequate. Research efforts to date have concentrated on gaining insights into the environmental implications of nanotechnology—for example with respect to fate, transport, and toxicological effects of ENPs—which currently lag behind production and application efforts [14]. Thus, the rapid increase in production of ENPs and ultimate incorporation into nano-enabled products has triggered a need for information on the potential environmental effects of nano scale pollutants. Such information is essential for the development of a sound risk assessment

framework, and in turn, can inform the adoption of safe-by-design approaches for future nano-enabled products.

Insufficient data and knowledge on the biological effects of ENMs has fostered the birth of nanotoxicology [3,15], initially focusing on establishing the effects of ENMs on humans [3,4,16,17,18]. Later, concerns began to emerge on the potential environmental effects of ENMs [2,19,20,21], leading to the development of nanoecotoxicology [22] as a branch of nanotoxicology chiefly focusing on the ecological health aspects of ENMs [22,23,24]. Fewer than 50 open peer-reviewed nanoecotoxicity studies had been reported by 2008 [17], when Klaine et al. [25] published a comprehensive review of nanoecotoxicology research. Since then, the number of published nanoecotoxicology studies has increased rapidly [14,22] and numerous excellent reviews focussing on the fate, behaviour, and toxic effects of ENPs have been published. Reviews cover the toxicity of ENPs to bacteria [26,27,28,29], algae [26,29,30,31], invertebrates [26,32,33,34,35] and fish [24,36,37,38], and the fate and behaviour of ENPs in aquatic systems (See Section 2). To the knowledge of the authors, no nanoecotoxicology review is available for aquatic higher plants, hence the focus of this article on the interactions of metal-based ENPs with aquatic higher plants.

Aquatic higher plants, also known as aquatic vascular plants include free floating or rooted, and emergent or submerged plants. Aquatic higher plants occupy a key position in ecological energy metabolism as producers and food source, and also shelter a variety of invertebrates [39]. Little nanoecotoxicity information is available for aquatic higher plants as opposed to micro-algal species and terrestrial higher plants, including agricultural crops [25,40,41,42,43,44]. The possibility exists that aquatic plants have the potential to bioaccumulate ENPs, and transfer them between trophic levels in aquatic ecosystems [45]. The assessment of the risk posed by ENPs in aquatic environments therefore requires data at different trophic levels [46]. Overall, this review on the interaction of ENPs with aquatic higher plants dealt with aspects of: (i) bioavailability, (ii) uptake, translocation and accumulation, and (iii) toxicity effects. The review generates an information portfolio on current

knowledge about the interactions of metal-based ENPs with aquatic higher plants. Furthermore, this review makes recommendations for future research directions that will help strategize and prioritize knowledge generation, through screening of patterns or commonalities in the current reported information.

BIOACCESSIBILITY

The interactions of ENPs with aquatic higher plants are complex and dynamic. Several key physico-chemical processes influence the amount and form of ENPs that interact with aquatic organisms including plants, as summarized here. Note that the concept of 'bioaccessible proportion' used in this article refers to the proportion of ENPs available for interacting with the plant surface, and potentially available for uptake [47].

The behaviour, fate and transport of ENPs in aquatic systems are influenced by their physical and chemical traits such as size, shape, surface charge potential, crystal structure, composition and surface coating. In aquatic systems, ENPs undergo numerous transformations as a result of biotic and abiotic factors which consequently determine ENPs' bioaccessibility, uptake, bioavailability and toxicity potential upon interaction with aquatic biota [48,49]. Therefore, aquatic biota encounter or interact with transformed rather than pristine ENPs, after release into aquatic environments [50,51]. Metal-based ENPs undergo a number of transformations in aqueous media (Figure 1). This review highlights the relevance of interactions of ENPs with aquatic plants, since the environmental behaviour of ENPs has been addressed in detail elsewhere [29,49,50,52,53].

For metal-based ENPs, one key determinant of their environmental fate is dissolution potential. The release of dissolved metallic forms or ions from metal-based ENPs is a chemical trait often enhanced with diminishing nano scale size, and which in turn increases their reactivity [52]. Thus, metal-based ENPs interact with biota in the following forms, namely: (i) dissolved metals, (ii) new chemical substances formed after interacting with biotic and abiotic aquatic factors, and, (iii) particulates [43]. Therefore, each study needs to pay attention to the bioaccessible fractions of metal-

based ENPs as a result of associated implications for uptake and toxicity. Already there are suggestions that uptake [42,45,54,55,56] and toxicity [44,53,57,58) of metal-based ENPs are dependent on their physico-chemical characteristics.

In aqueous suspension, metal-based ENPs often agglomerate, where gravitational forces may overcome buoyancy, causing sedimentation of particles and thereby reducing exposure concentration [29,44]. However, often overlooked is the opposite effect of de-agglomeration; as the transformation of ENPs is dynamic and multi-dimensional. Chemical processes such as reduction of metal cations (e.g. Ag^{+}) can result in the formation of smaller secondary particles in suspension [59], thereby introducing new bioaccessible size states. Changes in the size of ENPs are important for determining exposure size (bioaccessible size) and persistence in aqueous systems.

The interplay of agglomeration, de-agglomeration, sedimentation, and re-suspension of ENPs (Figure 1) has implications for free floating and rooted aquatic plants, causing spatial and temporal variation of exposure scenarios. Settling of ENPs onto sediments may purify aquatic systems of such contaminants [60], but this argument overlooks the fact that aquatic systems are not one-dimensional. For instance, during re-suspension ENPs can dissolve or de-agglomerate and still interact with pelagic biota. These and other case studies are discussed further in Sections 3 and 4, regarding their influence on uptake and toxicity. The physico-chemical properties of aquatic environments–such as pH, ionic strength, inorganic constituents, total organic matter–are important in the transformation of ENPs. These properties may alter bioaccessible size and surface properties, or influence dissolution rate. Transformations such as these exert influence on the bioaccessible state of ENPs to aquatic biota in general. Detailed accounts of the aquatic fate and behaviour of ENPs have been reported elsewhere [25,40,49,52,53,61,62,63,64], and are outside the scope of this article. Generally, the dissolution rate of metal-based ENPs is pH dependent [64,65], suggesting that varying pH regimes will present different bioaccessibility of ENPs to aquatic plants as well.

The toxicity of metals in aquatic environments is largely related to free metal activity or soluble metallic species [66]. Analysis of trace metal speciation involves the determination of metal chemical forms, including free metal ions, inorganic and organic complexes, and organometallic compounds. For instance, electrolytes and organic matter control the stability of ENPs as they interact with ENP surfaces, thereby altering surface characteristics such as surface charge potential and coating. When ENPs interact with aquatic higher plants, dissolved organic carbon (DOC) can increase the bioaccessible size of ENPs [42], as in the case of gold nanoparticles (nAu), where the resultant nAu–DOC complexes were larger than nAu and its homo-agglomerates, hence limiting uptake potential. Whether in particulate or dissolved form, ENPs interact with higher plants through processes such as adsorption, deposition and internalisation. The fate and toxicity implications have been discussed previously [49,67,68,69,70,71].

The above information suggests that the bioaccessibility and bioavailability of metal-based ENPs to aquatic higher plants is underpinned by a complex interplay of ENPs and exposure water characteristics. Therefore, integrating ENP characteristics and aqueous properties is necessary when investigating environmental behaviour of ENPs, rather than treating each component separately. Ultimately the bioavailability of ENPs in aquatic systems is determined by the complex interplay of processes highlighted earlier in this section, which are temporally and spatially dynamic. Factors influencing bioaccessibility of ENPs are fundamental because, in turn, they determine bioavailability, bioaccumulation, and toxicity towards aquatic higher plants.

ADSORPTION, UPTAKE, AND BIOACCUMULATION

Aquatic plants obtain essential nutrients from the surrounding aquatic matrices, so uptake of ENPs could arise from similar mechanisms [45]. Variability in ENP uptake mechanisms is likely because of physiological, anatomical and morphological diversity amongst aquatic higher plants. For instance, different uptake mechanisms can result from morphological differences in root [45] and vascular [72] systems between plant species. Herein, the term uptake broadly refers to processes by

which ENPs and their derivatives reach the inside of plant tissues or cells, through active and passive mechanisms. The term excludes adsorption onto plant surfaces. Therefore, bioaccumulation in this context can occur from internalised (uptake) or adsorbed ENPs and resultant dissolved metallic forms. The mechanisms reported in the context of ENPs association with aquatic higher plants are summarised in Table 1, excluding the bioaccumulation of dissolved metal forms. Bioaccumulation constitutes an important process during the interactions of ENPs with plants, as it can be a precursor to toxicological effects if the pollutant's concentration exceeds a certain threshold. Knowledge of uptake kinetics of ENPs by aquatic plants is incomplete, despite earlier research [41,43,72,73], although it is a key aspect that determines the bioavailability, bioaccumulation, and toxicity of ENPs.

Adsorption

Adsorption is a plausible mechanism for the accumulation of ENPs by aquatic higher plants [45,58,74,75). For example, electron microscopy techniques (transmission electron microscopy-TEM, scanning transmission electron microscopy-STEM and scanning electron microscopy-SEM) together with energy dispersive x-ray spectroscopy (EDX), showed the presence of gold nanoparticles (nAu) adsorbed on root tissue surfaces [45]. For *Egeria densa*, no internalisation of nAu was observed, which suggested that adsorption was likely the dominant accumulation mechanism, whereas for *Azolla caroliniana* and *Myriophyllum simulans* internalisation of nAu also occurred. The uptake of nAu was higher in *A. caroliniana* to *M. simulans*. This was attributed to the presence of stomata on both sides of fronds, as well as root hairs, which increase the surface area for uptake, whereas the other two species possess limited root hairs. The suggestion that uptake mechanisms differ between species [72] was supported by the findings of Glenn et al. [45].

Using electron microscopy techniques, Li et al. [74] found agglomerates of $nTiO_2$ adsorbed onto *L. minor* fronds but no internalisation was evident, and concluded that adsorption was the dominant accumulation mechanism in that investigation. The lack of $nTiO_2$ internalisation by *L. minor* was attributed to the sieving nature of the cell wall pores, and the sorption of ENPs to cell surface

exudates which in turn promoted agglomeration. Various epidermal structures and exudate forms (e.g. amino acids, enzymes or sugars) lining plant cell walls present a layer capable of further transforming ENPs (on interaction), and thus facilitate the uptake of ENPs, or even their rejection [76,77]. In addition, ENP internalisation through cell wall pores can be regulated by bioaccessible size [78]. Cell wall pores in plants are known to vary in size from about 10 to 50 nm [79,80,81]. Such size ranges raise the possibility that cell wall pores are capable of controlling entry, dependent on the exposure size and other characteristics [78]. However, in certain cases ENPs can penetrate cells even when they are larger than cell wall pore size, and these mechanisms are discussed in Section 3.2.

Adsorption to the root epidermis as well as tissue and cellular internalisation, were both found to result in the accumulation of copper oxide nanoparticles (nCuO) and cadmium sulfide quantum dots (CdS QDs) by *Schoenoplectus tabernaemontani* [75]. However, the predominant driver of the two processes was not determined. Furthermore, the contribution of dissolved metal forms to bioaccumulation was not investigated, and therefore the authors may have incorrectly associated bioaccumulation only with uptake of nano forms. Results indicated that accumulation of nCuO was rapid compared to CdS QDs, and hence uptake potential was ENP-type dependent, as earlier suggested [73,82]. However, Zhang et al. [75] did not account for the reported relatively higher nCuO accumulation compared to CdS QDs. We postulate that accumulation variability probably resulted from preferential assimilation of Cu released from nCuO, since Cu is an essential element in numerous physiological processes [83,84]. Dissolution analysis could provide more insight into this hypothesis. Internalisation of the ENPs was possibly facilitated by endocytosis [86,87] or carrier proteins [73,82,88]. Endocytosis is the active cellular internalisation of substances through engulfing by the membrane forming a vacuole. Following exposure of *Salvinia natans* to nZnO, adsorption of nZnO/Zn to roots was observed, but internalisation was not investigated [58]. Inductively coupled plasma-optical emission spectrometry (ICP-OES) was used to quantify Zn accumulated in unrinsed and rinsed roots,

where it was observed that rinsing resulted in Zn loss. Such findings provided confirmation of nZnO/Zn adsorbed to root surfaces.

Adsorption of ENPs to plant surfaces appears to be a key mechanism for their phytoextraction from surrounding water. For instance, some reports [45,58,74] have attributed accumulation of ENPs solely to adsorption while in other cases adsorption coupled with internalisation of nano and dissolved metal forms has been observed [45,75]. Adsorption can drive the accumulation of particulates and dissolved metallic forms from solution although such scenario has not been reported, it remains highly probable. This is not unexpected considering that accumulation of metallic species in any physico-chemical form will arise initially from physical contact with plant surface, thus rendering adsorption highly likely. The findings of Glenn et al. [45] and Zhang et al. [75] support this suggestion as ENPs were shown to be both inside (internalised) and outside (adsorbed) plant tissues.

Internalisation

Glenn et al. [45] reported nAu internalisation into the roots of *A. caroliniana*, and *M. simulans* while no uptake occurred in *E. densa.* Internalisation was found to vary with particle size and plant species. In *A. caroliniana* for instance, 4 nm nAu were detected at a higher frequency than 18 nm nAu, whereas no internalisation of 18 nm nAu was detected in *M. simulans*, thus illustrating size dependent internalisation, possibly due to cell wall pore size discrimination. Furthermore, relatively higher bioaccumulation of Au was observed in *A. caroliniana* while no uptake was detected in *E. densa.* Using TEM, they demonstrated the changes in root tissue density explained the differences in uptake among the three plants. As noted above, Glenn et al. [45] suggested the enhanced uptake of nAu by *A. caroliniana* was due to the presence of stomata on both sides of fronds as well as root hairs, which in turn increased the surface area for nAu uptake, unlike other species without root hairs. Secondly, higher uptake by *A. caroliniana* was also associated with its salt intolerance compared to the salt tolerant *M. simulans* and *E. densa*, where the latter species have the ability to efficiently control and limit uptake of substances from the surrounding water, including nAu in this instance. Higher nAu internalisation by

the salt intolerant *A. caroliniana* can be linked to carrier protein mediated internalisation (73,82), as carrier proteins in plants are active in osmoregulation. The differences in ENP uptake between species observed by Glenn et al. [45] illustrates the role of distinctive morphological and physiological characteristics between species, supporting earlier suggestions by Ma et al. [72].

Zhang et al. [75] investigated the internalisation of nCuO and CdS QDs in the roots of *S. tabernaemontani*. Presence of ENPs in epidermal tissue and within the plant cells was confirmed using electron microscopy techniques coupled with EDX. The internalisation of ENPs was partly ascribed to endocytosis considering that nCuO had a large size of 38 nm but was still detected inside the plant cells. Few reports have documented ENPs internalisation by aquatic higher plants (Table 1), nonetheless mechanisms underpinning internalisation of ENPs in plants remain poorly understood [41,81,89,90], a data gap that needs to be addressed in future investigations. Notably, there are suggestions that internalisation is mainly facilitated by processes similar to those for nutrients and moisture absorption from surrounding environment [91,92]. Others [78,91,93,94] have indicated that internalisation is facilitated by cell wall pores as they are semi-permeable, and therefore ENPs can pass into the cytoplasm. The cell wall pores are approximately (approx.) to be 10-50 nm in diameter [79,80,81], and as such can permit entry of substances from the environment, including ENPs, into the plant cells depending on bioaccessible size. However, small ENP size alone does not translate into cell wall pore internalisation [45,74,81], which points to other mechanisms facilitating internalisation.

For instance, endocytosis has been suggested to aid transferring of ENPs into plant cells [86,87), similar to facilitation of other substances into cells. This implies that endocytosis can also facilitate internalisation of ENPs larger than cell wall pores depending on particle properties and orientation [41,94]. However, the selectivity criteria is yet to be established [90]. Finally, binding of ENPs onto carrier proteins and organic chemicals has also been proposed [73,82,88]. For instance metallothioneins can facilitate assimilation of metal-based ENPs [90]. The size of ENPs size is a key determinant for their internalisation by aquatic higher plants [45]–smaller forms tend to be internalised

rapidly. Size is the only characteristic that has so far been reported to influence the internalisation of ENPs in nano form by aquatic higher plants. However, caution is raised against general assumption of higher internalisation rate for smaller ENPs solely based on their size. Rather, a complex set of plant characteristics, water physico-chemical parameters, and ENP properties that interactively determine internalisation potential. Internalisation kinetics is therefore a topic warranting further research.

Bioaccumulation and translocation

Bioaccumulation analysis is amongst the methods used in determining the bioavailability of metal-based ENPs to aquatic biota by quantifying biomass metal content. An example is the quantification of total Zn in plants after exposure to nZnO. Besides being an indicator of ENP bioavailability, bioaccumulation is a measure of the potential for bioconcentration and trophic transfer [45,95]. Bioaccumulation is also a potential method for phytoextraction of nano pollutants in wastewater treatment systems [75], an application commonly used for bioremediation of metal-contaminated waters [96,97]. Bioaccumulation remains a valuable indicator of metal contamination. Reports of metal bioaccumulation by aquatic higher plants exposed to metal-based ENPs are listed in Table 2. Importantly, bioaccumulation analysis will not normally reveal the underlying driving processes (uptake vs. adsorption), but assumptions can be derived from characterisation of ENPs, water chemistry, and knowledge of plant species physiology. Furthermore, discrimination between accumulation of dissolved metal forms and ENPs is often challenging, though dissolution analysis of the exposure water can provide insights into this aspect.

Zinc oxide nanoparticles (nZnO). In the study by Hu et al. [55], the duckweed *Spirodela polyrhiza* was exposed to nZnO (1 mg/L, 10 mg/L and 50 mg/L) and $ZnSO_4$ (3.5 mg/L) for 96 h. Zinc bioaccumulation in plants exposed to nZnO was directly related to exposure concentration. Whole plant Zn concentrations were approx. 2-4.5 mg/g from nZnO exposures, and 4.5 mg/g from soluble Zn exposure ($ZnSO_4$). Therefore, Zn bioaccumulation was rapid in soluble zinc exposures compared to nano counterparts. Dissolution analysis of nZnO indicated that Zn was predominantly bioaccessible in

the dissolved form as the ENPs rapidly agglomerated up to approx. 4 µm (average 130 nm). The larger particles were deemed too large for internalisation. Translocation assessment was not done because bioaccumulation analysis was performed on the whole plant [55].

Salvinia natans was exposed to 1 mg/L, 10 mg/L, 20 mg/L and 50 mg/L nZnO, and 44 mg/L $ZnSO_4$ for 7 d [58]. From nZnO exposures, Zn accumulation in leaves ranged from 0.45 to 3.65 mg/g, rinsed roots from 0.33 to 2.97 mg/g, and unrinsed roots from 0.49 to 8.18 mg/g. After $ZnSO_4$ exposure, Zn bioaccumulation was 4.28 mg/g in the leaves, 3.82 mg/g in the rinsed roots and 3.64 mg/g in the unrinsed roots. The results indicated higher bioaccumulation from $ZnSO_4$ than nZnO, when compared with 50 mg/L nZnO exposure. In the case of unrinsed roots, bioaccumulation was higher from exposure to nZnO than to $ZnSO_4$, and this pointed to the contribution of adsorbed ENPs. Large differences in bioaccumulation between rinsed and unrinsed roots exposed to nZnO are indicative of ENP adsorption onto root surfaces. After seven d, no suspended nZnO was detected in suspension of the testing medium because nZnO agglomerates sedimented to the bottom of the test vessel. Adsorption to root surfaces also contributed to the removal of nZnO in suspension. However, dissolution analysis confirmed the presence of dissolved Zn in the suspension of nZnO exposures. Therefore Zn accumulation was likely due to the adsorption of nZnO, adsorption and internalisation of dissolved Zn forms, with the latter process probably being predominant. Notably, internalisation of nZnO was unlikely, because of the formation of large agglomerates up to 1.6 µm in size, too large for cellular internalisation. Zinc content in the leaves and rinsed roots did not differ much although on average it was higher in the leaves. Such findings can erroneously be interpreted as indicative of active translocation of Zn from the roots to the leaves. This is because *Salvinia* spp. can absorb substances from water through their leaves as well as through their roots [98,99].

The reports on Zn bioaccumulation suggest that the process is directly related to exposure concentration and that the uptake rate for dissolved Zn is higher than for the nano counterparts. The uptake of nZnO is inhibited by transformations such as agglomeration.

Titanium dioxide nanoparticles ($nTiO_2$). Concentration dependent accumulation of Ti was reported after 7 d exposure of *Lemna minor* to 0.01-5 mg/L $nTiO_2$ [74]. Approximately an average of 70 mg/kg whole plant Ti was recorded at the highest exposure concentration compared to 0.37 mg/kg at the lowest exposure concentration. Electron microscopy analysis detected no internalised $nTiO_2$, pointing to adsorption as the main accumulation mechanism. Formation of larger $nTiO_2$ agglomerates (100-1000 nm) probably contributed to the lack of $nTiO_2$ internalisation. Translocation was not assessed because bioaccumulation analysis was undertaken for whole plant.

Oenanthe javanica and *Isoetes japonica* were exposed to 1.8 mg/L $nTiO_2$ (TiO_2-NP) and nanotube TiO_2 (TiO_2-NT) forms over 17 d [56] (illumination not reported). Bioaccumulation of Ti was analysed for whole body. After 17 d, the total accumulated Ti in *O. javanica* was 489.1 μg/g under TiO_2-NP exposure and 78.9 μg/g under TiO_2-NT exposure. For *I. japonica*, whole body Ti was 54.5 μg/g for TiO_2-NP exposure and 155.2 μg/g from the exposure with TiO_2-NT. No explanation was given to account for differences in accumulation of TiO_2-NP and TiO_2-NT, but the difference may lie in their distinctive morphologies, where orientation of TiO_2-NT at sites of contact limited the chance of internalisation. Translocation of Ti to the shoot system of *O. javanica* occurred, with Ti accumulation being 424.4 μg/g in the roots and 64.7 μg/g in the shoots under TiO_2-NP exposure. However, in exposures to TiO_2-NT, Ti concentrations were lower: 73.6 μg/g in the roots and 5.9 μg/g in the shoots.

Since $nTiO_2$ compounds are poorly soluble, researchers have considered interaction and bioaccumulation of $nTiO_2$ to be primarily driven by nano forms and have not performed dissolution analyses [56,74]. These studies also highlighted the role of ENP morphology [56] and exposure concentration [74] as factors influencing bioaccumulation by aquatic higher plants.

Copper oxide nanoparticles (nCuO). Perreault et al. [95] compared Cu bioaccumulation in *L. gibba* exposed to nCuO (0.68-4.51 g/L) and $CuSO_4$ (0.004-0.032 g/L) for 48 h. The rate of Cu accumulation was higher from $CuSO_4$ exposure compared to nCuO, and in both regimes it increased with increasing exposure dosage. It was hypothesized that Cu accumulation from nCuO exposures was

mainly in dissolved form as nCuO agglomerated rapidly in suspension. The same research group also investigated the influence of coating, concentration, and Cu form (particulate or dissolved) on the bioaccumulation of Cu by *L. gibba* [100]. The *L. gibba* was exposed to non-coated nCuO, styrene-co-butyl acrylate coated nCuO, and $CuSO_4$ for 48 h. In all exposures, whole body Cu increased with increasing exposure concentration. Furthermore, bioaccumulation concentration was established in the descending order as: $CuSO_4$ > coated nCuO > uncoated nCuO. These findings [100] suggested that dissolved Cu forms were rapidly accumulated as compared to nano counterparts. Dissolution of both nCuO forms was largely negligible, which pointed to accumulation arising from the particulate forms.

The coating of nCuO improved their uptake due to enhanced stability (retention of smaller sizes as coating inhibited aggregation) compared to uncoated forms which largely agglomerated (probably exhibiting higher settling rate), and in turn, limited their uptake. Polymer-coated nCuO were more toxic to micro algal species compared with uncoated nCuO [101], chiefly because the smaller coated nCuO were more able to interact and penetrate the cells than uncoated nCuO. Similarly, higher uptake of smaller-sized nAu by aquatic higher plants as a result of natural organic matter (NOM) steric stabilisation has also been reported [45]. Thus, the surface coating of ENPs appears to influence their accumulation by aquatic plants, although this will be subject to the activity of other water quality parameters. Studies on the exposure of *S. tabernaemontani* to nCuO (0.5 mg/L, 5 mg/L, and 50 mg/L) showed that Cu accumulation was dependent on both exposure concentration and duration [75]. After 21 d, at 50 mg/L, the roots accumulated Cu to more than 4000 µg/g and the shoots less than 20 µg/g, an indication of limited translocation from the roots to shoots. Internalised nCuO were detected in the epidermis and inside cells, hence Cu bioaccumulation probably resulted from adsorption and internalisation of both the nCuO particulates and dissolved Cu species.

Shi et al. [102] reported that *Landoltia punctata* accumulated approx. 700 µg/g Cu in the fronds and 800 µg/g Cu in the roots after exposure to 1 mg/L nCuO for 14 d. In the same study, the plants were exposed to 0.2 or 0.6 mg/L of dissolved Cu ($CuCl_2$). Bioaccumulation of Cu was approximately

<100 (fronds) and 300 µg/g (roots) from 0.2 mg/L exposure, whereas the 0.6 mg/L exposure yielded 500 (fronds) and 700 µg/g (roots). Although the findings appear to suggest higher assimilation rate of nCuO, the exposure concentrations of nCuO and $CuCl_2$ differed, making comparisons difficult. Bioaccumulation from nCuO exposures probably resulted from uptake of soluble Cu (based on dissolution findings), adsorption of nCuO, and maybe their internalisation as well. The findings further suggested transportation of Cu^{+}/Cu^{2+}/Cux/nCuO from roots to leaves, but there is need for caution, as leaves of this plant type are capable of absorbing nutrients from the surrounding environment.

Overall, the uptake of dissolved Cu appears to be the main driver of nCuO bioaccumulation based on findings of Perreault et al. [95,100]. Moreover, it can also result from the accumulation of both dissolved and particulate Cu forms [75]. Interestingly, the findings of Shi et al. [102] differ from those of Perreault et al. [95,100]. This is because accumulation of nCuO was reported to be higher than $CuCl_2$ exposures in Shi et al. [102]. However, the exposure concentrations of $CuCl_2$ (0.2 mg/L, 0.6 mg/L) and nCuO (1 mg/L) differed [102], which may have led to underestimation of soluble copper accumulation potential, and prohibits any meaningful comparison between accumulation of soluble Cu and nCuO.

Gold nanoparticles (nAu). Ferry et al. [103] demonstrated that *Spartina alterniflora* exposed to nAu rods for 12 d in an estuarine mesocosm had whole plant Au concentration of 3.45 µg/kg. The observed bioaccumulation was ascribed to adsorption of the insoluble nAu rods, which formed agglomerates that were deemed too large for internalisation. However, much higher Au accumulation by *S. alterniflora* occurred during 11 d exposure to nAu rods under similar estuarine mesocosm conditions [104]. Bioaccumulation of Au in the roots was 117 µg/kg (more than 30 times that reported by Ferry et al. [103]), 4.42 µg/kg in stems and 11.3 µg/kg in aerial parts. Exposure concentrations were 7.08×10^8 particles/mL in Ferry et al. [103], 3.42×10^7 particles/mL in Burns et al. [104], so the cause for much higher bioaccumulation is unclear.

The higher Au accumulation in the roots was associated with adherence of sediment particles to the roots, even though the roots were washed to remove sediment particles [104]. Bioaccumulation analysis also indicated probable active translocation of Au from roots as sites of uptake through stems where accumulation was less, to aerial parts where deposition was more than double that in the stems. As a member of the Poaceae family, absorption of nutrients in *S. alterniflora* is primarily a function of the roots, because a thick cuticle to reduce water loss in stems and shoots inhibits this function [45]. Bioaccumulation rates of nAu may be dependent on ENP size and the plant species [42,45]. For example, higher Au accumulation was observed from 4 nm nAu compared to 18 nm nAu across all plant species [45]. *A. caroliniana* accumulated in excess of 120 mg/kg Au from 4 nm exposure and less than 60 mg/kg from 18 nm nAu exposure. Similar trends were observed in other experiments, where less Au bioaccumulation was found in plants exposed to 30 nm nAu than to 4 or 18 nm nAu [42]. Such nAu accumulation patterns were ascribed to relatively higher internalisation rates of smaller nAu particulate forms, for instance, by *M. simulans* and *A. caroliniana* [45].

Conversely, no nAu internalisation was found in *E. densa*, so the observed bioaccumulation was wholly attributed to adsorption of ENPs, because dissolution was insufficient for appreciable internalisation of soluble Au. In both studies [42,45], Au accumulation was highest in *A. caroliniana*, moderate in *M. simulans* and lowest in *E. densa*. The interspecies differences were attributed to varying morphological and physiological characteristics between the species. Moreover, bioaccumulation of Au was found to be influenced by water chemistry, namely NOM concentration [42]. Addition of NOM inhibited accumulation due to the formation of nAu-DOC complexes that were larger than the cell wall pores, resulting to reduced potential for nAu uptake. Although no uptake was observed due to nAu-DOC complex formation, nAu stability was enhanced, an effect that could extend their persistence in the environment.

Generally, poor solubility of nAu suggests that their bioaccumulation by aquatic higher plants is mainly through accumulation of nano particulates. This means it is mostly influenced by characteristics

of nAu, and exposure media properties. For instance, the role of bioaccessible size is evident in reports from Klaine's research group [42,45], but varies between plant species and physico-chemical conditions of the exposure medium. The role of roots in nutrient absorption also facilitates accumulation of nAu, because the Au content in roots was high. Depending on the plant species, nAu can be translocated to aerial tissues as well.

Silver nanoparticles (nAg). Spirodela polyrhiza was exposed to nAg and $AgNO_3$ (0.5–10 mg/L) for 72 h in a study by Jiang et al. [54]. The bioaccumulation of Ag from both Ag forms was dependent on exposure concentration, and was much higher in plants exposed to $AgNO_3$. After 72 h at 10 mg/L exposure dosage, the average Ag bioaccumulation from nAg was below 4 mg/g but above 10 mg/g from $AgNO_3$ [54]. The findings suggest that bioaccumulation of soluble Ag was rapid compared to nAg, similar to other ENPs reported earlier in Sections 3.3.1 and 3.3.3. Other reports on Ag have associated their interactions with aquatic biota with the formation of soluble Ag species [105,106], so adding dissolution analysis to the procedure of Jiang et al. [54] would help elucidate probable mechanisms for nAg bioaccumulation. Higher accumulation of Ag from $AgNO_3$ exposures may be linked to its higher solubility, thus enhancing internalisation, unlike nAg, which has low solubility [44,107]. This hypothesis appears plausible based on the generally low solubility of nAg [44,107,108]. No translocation data is available because whole plant Ag accumulation was undertaken in the studies of Jiang et al. [54].

Lemna gibba exposed to nAg for 7 d accumulated Ag dependent on exposure concentration, ranging from 7.72 to 17.5 µg/mg under exposure to nAg concentrations of 0.01 to 10 mg/L [107]. Bioaccumulation was mainly associated with internalised nAg, since the plants were washed with chelating ethylenediaminetetraacetic acid (EDTA) and dissolution was approx.1% of nominal dose. However, no plant cross sections were examined with electron microscopy to assess internalisation of nAg. Based on the nAg hydrodynamic size distribution (159–447 nm), the agglomerates appeared too large for Ag bioaccumulation to be largely attributed to nAg internalisation. Therefore, it is likely that

the adsorbed nAg and dissolved Ag forms accounted for the reported bioaccumulation, since no evidence was presented suggesting complete removal of adsorbed nAg/soluble Ag after washing with EDTA. Thus, the analysis of plant cross sections with electron microscopy would have offered useful insights into the hypothesis of nAg internalisation suggested by Hund-Rinke et al. [13].

The reports on Ag bioaccumulation following nAg exposure suggest that the process is dependent on exposure concentration, and that accumulation of dissolved Ag forms is rapid relative to nano counterparts. Other than the release of soluble forms, other mechanisms for nAg bioaccumulation are yet to be explored in detail. For instance, adsorption and internalisation of nAg are yet to be reported, including the ENPs characteristics that can influence such bioaccumulation mechanisms. Bioaccumulation of nAg is likely to be size dependent, being greater at smaller sizes as a result of raised potential for dissolution, internalisation, and adsorption.

Cadmium sulphide quantum dots (CdS QDs). The bioaccumulation of Cd by *S. tabernaemontani* depended on exposure duration and concentration in plant roots and shoots following 21 d exposure to 0.5 mg/L, 5 mg/L, and 50 mg/L CdS QDs [75]. Bioaccumulation of Cd in the roots (approx.1500 µg/g) was 190-fold higher than in the shoots (approx.8 µg/g), which indicated limited translocation from roots to shoots. Both adsorption and internalisation of CdS QDs were evidently accumulation drivers, with the former being dominant due to the association of nanoparticles with the roots.

Summary: bioaccumulation and translocation. Accumulation of ENPs by aquatic higher plants is complex, with environmental parameters and ENP transformations interacting to influence the uptake process (Table 1 and 2). Reports of ENPs internalisation were few (Table 1), probably because of the difficulty associated to tissue sample preparation and the specialised analytical equipment required. Differentiating between internalisation and adsorption of ENPs provides useful information for hazard and bioavailability assessment exercises. However, for trophic transfer and phyto-extraction evaluation, such discrimination is of limited value. Total metal bioaccumulation has predominantly

been utilised as an indicator of ENP accumulation (Table 2), most likely because of the simpler analytical protocol and more accessible analytical equipment required, such as inductively coupled plasma (ICP) optical emission spectroscopy or ICP mass spectroscopy. Generally, bioaccumulation depended on exposure concentration and ENP size, influenced by ENPs surface chemistry/coating. Bioaccumulation of soluble metal forms was higher than for nano particulates. Furthermore, adsorption of both the dissolved and nano metallic derivatives contributed notably to bioaccumulation. The bioaccumulation of bulk scale metals by aquatic biota is apparently related to exposure concentration, but the bioconcentration factor is inversely related to exposure concentration for chronic exposures [109]. Therefore, metal bioaccumulation resulting from metal-based ENPs reviewed here is in agreement with trends for bulk scale counterparts. Predictions about the predominant driver of bioaccumulation between metallic particles and soluble metallic forms were mostly founded on dissolution analysis of the exposure water. The solubility of ENPs appear to influence bioaccumulation as enhanced bioaccumulation tended to be associated to higher solubility, thus suggesting lower uptake potential for ENPs relative to soluble metal derivatives.

TOXICITY EFFECTS

A growing body of scientific literature describes the toxicity of different classes of ENPs such as metals [44,54,105,108], metal oxides [44,55,58,110], and quantum dots [75] to aquatic higher plants. For simplicity, in this review, the toxicological end-points are categorized as subcellular (oxidative stress and damage), photosynthetic (chlorophyll pigments and photosynthetic activity) and growth (biomass and growth rate) effects.

Subcellular

The sub-cellular category of effects consists of endpoints such as activity of antioxidants, oxidative damage and protein content. Findings on subcellular effects of metal-based ENPs to aquatic higher plants, and relative exposure conditions are summarised in Table 3.

Copper oxide nanoparticles (nCuO). Forty-eight h exposure of *L. gibba* to $CuSO_4$ (0.004-0.032 g/L), polymer coated nCuO (0.25–1.24 g/L) and bare nCuO (0.68–4.51 g/L) inhibited esterase enzyme activity and enhanced generation of reactive oxygen species (ROS). The effects were dependent on exposure concentration [100]. The ROS generation per viable biomass was in the order: $CuSO_4$ > coated nCuO > uncoated nCuO. However, ROS formation based on soluble Cu fractions and Cu bioaccumulation was coated: nCuO > uncoated nCuO > $CuSO_4$. The findings suggested that for nCuO ROS generation, the basis was nano driven compared to soluble Cu as the latter was less oxidative, and such findings were attributed to rapid uptake of the coated and more stable nCuO. On the activity of esterase enzyme, the effect was $CuSO_4$ > uncoated nCuO > coated nCuO. The findings for the esterase enzyme indicated that soluble Cu was highly toxic to the nano counterparts. The investigation [100] suggested that toxicity of nCuO is dependent on the endpoint being assessed, and solubility potential. Further studies will improve our understanding of the difference in toxicological potency between nCuO and soluble Cu.

Titanium dioxide nanoparticles ($nTiO_2$). Song et al. [110] investigated the induction of oxidative stress to *L. minor* following exposure to bulk and nano forms of TiO_2 (10–2000 mg/L). There was activation of peroxidase (POD), catalase (CAT), and malondialdehyde (MDA) in plants exposed to $nTiO_2$ across exposure concentrations. Bulk TiO_2 was generally toxic at high exposure concentrations, for instance, it only activated POD and superoxide dismutase (SOD) at 2 g/L, and CAT at 1–2 g/L. The results pointed to higher toxicity of $nTiO_2$ compared with bulk counterparts, a size dependent phenomenon. It can be assumed that there was better uptake of $nTiO_2$, but also that bulk TiO_2 rapidly settled out of suspension due to its size. The investigators did not account for possible differences between the toxicity of $nTiO_2$ and bulk TiO_2. However, it also is plausible that photo-activation of $nTiO_2$ was enhanced compared to larger counterparts.

Zinc oxide nanoparticles (nZnO). The activities of CAT, POD, SOD, and Na^+K^+ATPase were assayed in *S. polyrhiza* following 96 h exposure to nZnO (1–50 mg/L) and $ZnSO_4$ (3.5 mg/L) [55]. All

endpoints were significantly altered by $ZnSO_4$, where it stimulated CAT and SOD but inhibited POD and Na^+K^+ATPase. For nZnO, Na^+K^+ATPase was insignificantly influenced and SOD activity increased by ≥10 mg/L, whereas both CAT and POD were only significantly stimulated at the highest exposure concentration. Both SOD and CAT activities were stimulated by 10–50 mg/L of nZnO as well as exposure to $ZnSO_4$. Conversely $ZnSO_4$ inhibited the POD and Na^+K^+ATPase, but nZnO only inhibited POD at the highest concentration. When comparing similar exposure concentrations, dissolved Zn ($ZnSO_4$) was more toxic than nZnO. Due to the agglomeration of nZnO, the dissolved Zn derivatives were postulated as the underlying cause of the observed toxicological effects following nZnO exposures. Immediate agglomeration (approx. average 0.3 µm) at 0 hrs occurred, leading to sedimentation. No nZnO was detected in suspension after 12 hrs. Similarly, in a study by Hu et al. [58], dissolved Zn was raised as the dominant cause of toxicity to *S. natans* exposed to nZnO (1–50 mg/L) and $ZnSO_4$ (44 mg/L) for 7 d. nZnO activated SOD at 10–50 mg/L and CAT at 50 mg/L, inhibited POD at 50 mg/L, and was not toxic to Na^+K^+ATPase. The $ZnSO_4$ activated SOD and CAT, but inhibited POD and Na^+K^+ATPase [58].

Thwala et al. [44] exposed *S. punctuta* to nZnO (0.01–1000 mg/L) for 14 d, and the results revealed induction of various forms of oxidative imbalances. The observed effects exhibited both temporal and dose dependency. For instance, the production of reactive oxygen and nitrogen species (ROS/RNS) evaluated by the 2',7'-Dichlorodihydrofluorescein (DCF) method at the highest exposure concentration was below 1.5 nM after 4 d but reached 175 nM after 14 d. Furthermore, minimum ROS/RNS production of approx. 25 nM was observed at 0.01 mg/L nZnO and increased to 175 nM at 1000 mg/L nZnO, indicating that free radical production was dose dependent. Similarly, hydrogen peroxide (H_2O_2) and total antioxidant capacity (TAC) were much higher after 14 d than after 4 d exposure. However, similar SOD activity was observed at the highest exposure concentration regardless of exposure duration. The effects were associated with the dissolved Zn based on the dissolution data: at the highest exposure concentration, the dissolved Zn concentration after 4 d was 12

mg/L and after 14 d, 13 mg/L, which may account for the similarity in SOD activity irrespective of the exposure period. The nano counterparts underwent rapid agglomeration, reaching sizes of up to 1350 nm, and settled out of suspension.

Silver nanoparticles (nAg). Jiang et al. [54] reported that *S. punctata* experienced significant reduction of total nitrate-nitrogen, phosphate-phosphorus, and carbohydrate after exposure to 0.5–10 mg/L of nAg and $AgNO_3$. The effects were exposure concentration dependent. Similarly, proline production, an indicator of stress, increased with increasing exposure concentration. The $AgNO_3$ had greater toxic effects than nAg, suggesting that the toxicological potency of dissolved Ag is higher than the nano forms. Dissolution analysis would be required to accurately establish whether the underlying driver of nAg toxicity was dissolved or nano Ag. However, nAg exhibit slow dissolution [44,107,108], therefore their toxicity was probably a nano effect. Free radical production in *S. punctata* was nAg dose dependent [44] and declined at higher concentrations owing to the reduction in biomass, with 100% mortality at the highest exposure concentration. The observed SOD activity inhibition due to nAg was postulated to be as a result of protein denaturation after oxidative damage. The dissolution of nAg was virtually negligible (below detection after 14 d at the highest concentration), so dissolved Ag species had very little influence on the observed toxicity [44]. *Lemna gibba* exposed to 0.01–10 mg/L nAg for 7 d [107] showed free radical activity assayed by DCF fluorescence, which increased with increasing exposure concentration. Cell viability was also affected by nAg where the percentage of viable cells initially increased at the lowest dosage but significantly decreased at all other exposure dosages. Based on low solubility of nAg, the dissolution of internalised nAg was most likely the main driver of the toxic effects [107].

Jiang et al. [108] reported size dependent toxicity of nAg on *Spirodela polyrhiza* following exposure to average 6 nm nAg (0.5–10 mg/L), 20 nm nAg (10 mg/L), and > 1 μm Ag (10 mg/L) for 72 h. The endpoints assayed were ROS content, SOD, CAT, POD, MDA, GSH, and protein content. The ROS content was raised by 6 nm nAg (≥ 0.5 mg/L) and 20 nm nAg, but not by bulk Ag. All nAg forms

increased SOD activity, but this was not the case with bulk Ag. CAT activity and MDA content were raised only by 5 mg/L with exposure to 6 nm nAg. Exposure to 5–10 mg/L of 6 nm nAg, and also 20 nm nAg increased POD activity. Protein content was elevated by 1–5 mg/L of both the 6 nm and 20 nm nAg. Lastly, the GSH content was increased by 6 nm nAg (≥ 1 mg/L), 20 nm nAg, and bulk Ag. Therefore, bulk Ag was toxic to GSH only, and none of the other endpoints. Dissolution of nAg was slower than that of bulk-Ag – which suggested that nAg toxicity was mainly nano driven. The contradiction between the two studies [54,108] results from the fact that $AgNO_3$ was used in the former [54], whereas micron size Ag was used in the latter [108], hence the Ag derivatives were chemically different.

Photosynthetic effects

Grouped under photosynthetic effects were endpoints associated with the functioning of the photosynthetic pathway. Table 4 provides a summary of findings on the photosynthetic effects of metal-based ENPs to aquatic higher plants.

Copper oxide nanoparticles (nCuO). The effects of nCuO (0.7–4.5 g/L) and $CuSO_4$ (0.004–0.032 g/L) on the photosynthetic system of *L. gibba* were reported by Perreault et al. [95]. Both nCuO and $CuSO_4$ inhibited Photosystem II (PSII) activity, and the toxicity of the Cu salt was greater than that of its nano counterparts. Various endpoints were assayed to assess the effects on the energy fluxes in the photosynthetic membrane. Both Cu forms reduced the number of active PSII reaction centres per chlorophyll unit, and further affected PSII yield similarly. The toxicity of the nCuO was mainly associated with the release of dissolved Cu forms *Lemna gibba* exposed to bare nCuO (0.68–4.51 g/L), polymer-coated nCuO (0.25–1.24 g/L), and $CuSO_4$ (0.004–0.032 g/L) [100] had PSII inhibited in all exposures, and toxicity was shown to be exposure concentration dependent. Soluble Cu was more toxic than either nano form, where the bare-nCuO were the less toxic of the nano form. The findings were attributed to rapid uptake rate of soluble Cu, and coated nCuO being more stable than uncoated nCuO which were observed to agglomerate rapidly.

Shi et al. [102] exposed *L. punctata* to nCuO (1 mg/L) and $CuCl_2$ (0.2 and 0.6 mg/L) for 14 d. The Cu salt reduced chlorophyll content (Chl *a, b, a+b*) in a concentration dependent manner. It was unclear which of the two Cu derivatives was more toxic since the exposure concentrations differed. The solubility of nCuO was 0.16 mg/L, which suggested that its toxicity was mainly nano driven. From the $CuCl_2$ exposures; the dissolved Cu was determined to be 0.2 mg/L and 0.6 mg/L. Although copper is an essential element in plant physiology, when in excess it inhibits photosynthesis, especially PSII [111].

Titanium dioxide nanoparticles ($nTiO_2$). Exposure of *L. minor* to $nTiO_2$ (10–2000 mg/L) caused an increase of chlorophyll content in a dose dependent trend, but no effects were observed following exposure to bulk-TiO_2 [110]. Such findings were suggestive of size influenced toxicity of TiO_2. The 200–2000 mg/L concentrations of $nTiO_2$ significantly increased chlorophyll content. The effect of $nTiO_2$ of increasing chlorophyll content appeared to enhance photosynthesis, whereas an inhibition effect would generally be expected. This was puzzling because growth inhibition was observed at similar exposure concentrations. The reason for such observations was not investigated. The chlorophyll content in *L. minor* exposed to 0.01–5 mg/L $nTiO_2$ remained similar to that of control samples [74]. The lack of negative effects on Chl *a* was attributed to the lack of $nTiO_2$ internalisation, suggesting it was not bioavailable to the plants. In summary, both studies [74,110] appear to suggest that the negative effect on Chl *a* in *L. minor* would only occur at very high concentrations, which are not environmentally realistic.

Aluminium oxide nanoparticles (nAl_2O_3). Aluminium oxide nanoparticles increased the photosynthetic efficiency of *L. minor* [112], but the effect was not exposure concentration dependent. The photosynthetic efficiency measured as PSII quantum yield and photochemical quenching increased as the exposure concentrations increased, and were more significant at higher exposure concentrations. However, non-photochemical quenching was least at higher concentrations.

Zinc oxide nanoparticles (nZnO). Spirodela polyrhiza was exposed to nZnO (1–50 mg/L) and $ZnSO_4$ (3.5 mg/L) for 96 h [55]. Only the 50 mg/L nZnO reduced the Chl *a* to phaeophytin ratio, whereas $ZnSO_4$ was inhibitive at 3.5 mg/L. Thus, soluble Zn ($ZnSO_4$) was highly toxic compared to the nano derivatives. The toxicity of nZnO was associated with its dissolution because it underwent aggregation under the exposure conditions. Hu et al. [58] exposed *S. natans* to 1–50 mg/L nZnO and 44 mg/L $ZnSO_4$. Assay results for Chl *a, b* and carotenoid indicated $ZnSO_4$ inhibited all the endpoints, however nZnO only inhibited the chlorophylls at the highest exposure concentration. Similar to the findings of Hu et al. [55], $ZnSO_4$ was more toxic than nZnO to *S. polyrhiza* when compared at similar exposure concentrations. Therefore, the two studies [55,58] collectively point to dissolution driven toxicity of nZnO.

Silver nanoparticles (nAg). Exposure of *S. polyrhiza* to nAg and $AgNO_3$ (0.5–10 mg/L) for 96 h reduced Chl *a*, Chl *a*/Chl *b*, and also photochemical efficiency ratio. The effect was exposure concentration dependent [54]. Although $AgNO_3$ seemed relatively more toxic, the authors argued that the toxicity of the two Ag forms was generally similar; however, sensitivity varied between toxicity endpoints. Following low Ag bioaccumulation in nAg exposures [54], it can be hypothesized that if uptake of nAg was increased likewise, the toxicity of nAg would likely be higher than that of $AgNO_3$ based on mass/volume exposure concentrations. This case further indicates the need for more detailed information on the uptake kinetics of ENPs by aquatic higher plants. For instance, future studies need to consider whether linkages exist between the toxicity effects and accumulation of ENPs.

Growth effects

The effects on plant growth parameters are presented in this section. Table 5 summarises findings from investigations of metal-based effects on aquatic higher plants.

Copper oxide nanoparticles (nCuO). Lemna gibba exposed to $CuSO_4$, bare nCuO and polymer coated nCuO for 48 h experienced growth inhibition from all the Cu exposures [100]. The toxicity was ranked as $CuSO_4$ > polymer coated nCuO > bare nCuO, where the latter caused the least growth

inhibition. The results indicated higher toxicity of soluble Cu in comparison to nano particulates, as the former underwent higher accumulation rate. The polymer coated nCuO were more inhibiting compared to bare nCuO, and the effect was suggested to be due to polymer alteration of cellular interaction and higher stability which in turn enhanced uptake and toxicity. Also in the findings of Perreault et al. [95], soluble Cu ($CuSO_4$) was more growth inhibiting than nCuO towards *L. gibba*, following a 48 h exposure. The toxicity of nCuO was attributed to the release of soluble Cu, considering that nCuO rapidly agglomerated and settled at bottom of test vessel at higher rate.

In another study, the growth effects of $CuCl_2$, nCuO and bulk CuO in *L. punctata* were studied for 96 h [102]. Frond numbers were most reduced by the Cu salt and nCuO, while bulk CuO was the least toxic form. Bulk CuO was less toxic than nCuO, as the latter was approx. 14 times more soluble than the latter. A comparative study [102] between $CuCl_2$ (0.2 mg/L, 0.6 mg/L) and nCuO (1 mg/L) on frond doublings and numbers, indicated that nCuO had similar toxicity to 0.6 mg/L of $CuCl_2$. The toxicity of $CuCl_2$ was observed to be exposure concentration dependent. The authors suggested that nCuO were less soluble than $CuCl_2$ and agglomerates were probably too large for internalisation, and thus adsorbed onto plant surfaces, while dissolved Cu were likely released from adsorbed nCuO fractions. Zhang et al. [75] exposed *S. tabernaemontani* to nCuO (0.5-50 mg/L) and Cu^{2+} (0.06 mg/L) for 21 d. Plants exposed to 0.5 and 50 mg/L nCuO, respectively, had 9 and 18% biomass reduction after 21 d. However, exposure to either nCuO or Cu^{2+} did not significantly reduce biomass compared to the control population, but nCuO appeared more growth inhibiting than Cu^{2+}.

Silver nanoparticles (nAg). Gubbins et al. [113] investigated the growth effects of two sizes of nAg (29, 93 nm), and $AgNO_3$, using exposure concentrations of 5–160 µg/L for up to 14 d. Frond number, biomass (dry weight), and relative growth were assayed in the investigation. The toxicities of both nAg forms, and $AgNO_3$ on *L. minor* were dependent on exposure concentration and duration. The toxicity of soluble silver ($AgNO_3$) was higher compared to 29 and 93 nm nAg counterparts. The relatively higher toxicity of $AgNO_3$ was linked to predominating soluble Ag compared to nAg

exposures, where solubility was found to be < 1% of exposure dosage. Hence, it was suggested that the uptake rate of dissolved Ag forms was higher than that of nAg, which accounted for the higher toxicity potential. Notably, no size induced toxicity differences were reported between nAg batches averaging 29 and 93 nm [113].

Similarly, $AgNO_3$ was more growth inhibiting than nAg to S. *polyrhiza* following 72 h exposure at 0.5–10 mg/L concentrations [54]. The observation was attributed to higher uptake and accumulation of dissolved Ag from $AgNO_3$ exposure whereas the dissolution of nAg was <3% of the initial dose. Another investigation [114] similarly reported growth effects of nAg on *L. minor* as exposure concentration and duration dependent in 8–128 µg/L for 7 d. Frond numbers and growth rate were assayed in their study. However, no elaboration on underlying mechanisms for the toxicity observed was provided. Kim et al. [115] also reported exposure concentration dependent growth inhibition of *Lemna paucicostata* exposed to 0.1–200 mg/L nAg for 7 d. At test end, nAg concentration in a range of 1–50 mg/L significantly reduced *L. paucicostata* growth rate, with complete inhibition at ≥100 mg/L. In this study [115], there were no attempts to define the mechanistic drivers of the observed nAg effects. However, a loss of total Ag in suspension after prolonged exposure was reported and was hypothetically linked to nAg agglomeration. In the investigation by Oukarroum et al. [107] where *L. gibba* was exposed to nAg (0.01–10 mg/L) for 7 d, frond number and growth were inhibited in a concentration dependent manner. The results indicated that nAg reduced both growth and number of fronds due to cellular solubilisation of internalised nAg, which in turn increased free radical activity and decreased free cellular viability. Dissolution of nAg appeared insignificant. After 24 h at 10 mg/L soluble Ag was recorded at a mere 0.15 mg/L, although more soluble Ag could be released as the study progressed. Therefore nAg toxicity was mostly probably nano driven.

Titanium dioxide nanoparticles ($nTiO_2$). Lemna minor exposed to 0.1–5 mg/L $nTiO_2$ for 7 d did not exhibit growth effects when assayed for growth rate and frond number [74]. Agglomeration and loss of $nTiO_2$ in suspension were argued as basis for reduced bioavailability, and probably toxicity

reduction. The authors [74] suggested the lack of toxicity effects (photosynthetic and growth related) were as a result of poor $nTiO_2$ uptake as evidenced by electron microscopy-based results, indicating no internalised $nTiO_2$. Because $nTiO_2$ is poorly soluble; its effects are probably due to nano particulates activity. Results of Kim et al. [115] showed $nTiO_2$ at 250 and 500 mg/L significantly inhibited *L. paucicostata* growth rate after 7 d. The induction of toxicity effects with increasing exposure dosage was suggested to be a result of an increasing accumulation rate of $nTiO_2$. Although ENPs tend to agglomerate with increasing concentration, leading to precipitation and sedimentation, in some instances increasing exposure concentration can promote adsorption of ENPs onto plant surfaces.

Aluminium oxide nanoparticles (nAl_2O_3). Juhel et al. [112] exposed *L. minor* to up to 10 mg/L nAl_2O_3 for 7 d and observed growth stimulation. The effect was linked to a "nano" effect after assessment of bulk aluminium, which was found not to be growth inhibiting. The growth stimulation was not associated with Al^{3+} ions released due to nAl_2O_3 dissolution, but partly as a result of enhancement of photosynthetic efficiency and root length, probably a counter-stress mechanism. The details on the mechanistic growth stimulation by nano alumina remain unclear and require further investigation.

Zinc oxide nanoparticles (nZnO). Overall toxicity of $ZnSO_4$ (3.5 mg/L) on *S. polyrhiza* was found to be higher than for nZnO (1–50 mg/L), due to its elevated inhibition on growth rate, frond number, and biomass [55]. The higher solubility of $ZnSO_4$ than nZnO, allowing more rapid uptake, was put forward as the reason for the former being more toxic. It was suggested that agglomeration led to a reduction of nZnO bioavailability in suspension, consequentially suppressing bioavailability and toxicity. Higher growth effects of $ZnSO_4$ relative to nZnO have also been reported by others [58]. No significant growth effects were observed in *S. natans* exposed to nZnO, whereas $ZnSO_4$ caused growth inhibition [58]. Both studies suggested that $ZnSO_4$ was more soluble that nZnO, hence the former was more bioavailable and toxic [55,58]. Note that the studies used different exposure media.

Cadmium sulphide quantum dots (CdS QDs). Following 21 d' exposure to CdS QDs (0.5–50 mg/L), *S. tabernaemontani* experienced biomass reduction, and the effect was found to be dosage dependent [75]. The plants had 31% biomass reduction at an exposure concentration of 5 mg/L and 44% at 50 mg/L. The toxicity of CdS QDs was hypothesized to arise from interactions with CdS QDs and dissolved Cd, but it is unclear which was predominant.

Summary: toxicity effects. The toxicity literature reviewed here points to the toxicity of metal-based ENPs as a result of soluble metallic forms, or nano forms, or even both. When compared at similar exposure concentrations, soluble metallic forms are rapidly accumulated and therefore more toxic than nano forms. Notably for both forms, the toxicity is directly related to exposure concentration. As a key discriminator between metal-based ENPs and other types of ENMs, solubility seems to be an important regulator of their toxicity. Therefore, relatively soluble ENPs (e.g. nZnO) tend to be more toxic than poorly soluble forms (e.g. $nTiO_2$). However, one should treat such generalisations with caution. For instance, when it comes to oxidative stress endpoints, the toxicity of nano forms tends to be higher than for their soluble counterparts, especially for poorly soluble ENPs such as nAg and $nTiO_2$. It is also important to factor in persistent and slow release of soluble forms by ENPs, when assessing the hazard of nano versus soluble metal forms. Furthermore, size, surface chemistry and other characteristics of ENPs may influence their toxicity potential.

No reports investigated the additional influences of exposure and environmental water physico-chemical conditions. The effect of photoactivity of $nTiO_2$ on aquatic higher plants is another gap in the literature requiring attention because of its effects on the photosynthetic pathway.

SUMMARY AND FUTURE PERSPECTIVES

This review suggests that the interactions of ENPs with aquatic higher plants are influenced by the interplay of numerous parameters under three broad categories: characteristics of ENPs, environmental water properties, and plant characteristics (physiological and anatomical). Diverse experimental protocols and instrumentation were adopted in the reviewed investigation (Tables 1–5),

and commonalities among the protocols were rare. This raises challenges regarding data comparability, uniformity, and usability. Therefore, we recommend the development and adoption of standardized testing protocols in order to identify key focus parameters, and improve data comparability to enhance the quality of data that supports risk assessment of ENPs detrimental to aquatic higher plants. Despite these misgivings, we provide the following salient perspectives of the current information portfolio, with the hope that they will also contribute towards harmonisation of test protocols.

- Smaller ENPs tend to possess higher uptake potential by plants and in turn higher toxicity than their larger counterparts do, as demonstrated in numerous studies reviewed. The main controlling factors are the complex dynamics of bioavailability linked to ENPs' size and exposure media chemistry. The bioavailable size at the site of interaction matters more than the ENPs' primary size. Small ENP bioavailable size alone does not imply effective uptake because plant physiological and phenotypic characteristics may also influence uptake. Collectively, the findings suggest a higher risk potential towards aquatic plants from smaller ENPs, due to enhanced bioaccumulation and toxic effects. Besides the size of ENPs, their morphological and surface properties (e.g. coating) can significantly influence their interactions with aquatic higher plants. However, details of these aspects are still required for an understanding of the physico-chemical basis for the effects of surface coating and morphology. For instance, electron microscopy images can better illustrate the dynamics of interaction at plant surface, and tissue or cellular internalisation, as a factor of ENPs morphology. Therefore, investigations on the role of ENPs morphology on uptake by plants are encouraged.

- Current data suggests that exposure concentration influences ENPs bioaccumulation and toxicity effects, generally in a direct proportional relationship. However, reporting of actual exposure concentrations as total or dissolved metal per volume or particle number per volume was often poor. This aspect is important for hazard evaluation and determination, because dissolution and agglomeration of ENPs can alter exposure

concentration. Therefore, future studies should carefully evaluate ENPs dissolution to improve data quality, and in turn, the nature and extent of conclusions drawn. For instance, dissolution of metal-based ENPs regulates their interaction with aquatic plants, as internalisation and accumulation rates from exposure to soluble metallic forms are often higher than from exposure to colloidal nano forms. Even when higher accumulation resulted from ENPs exposure, this was ascribed to higher dissolution rate of nano forms. Hence, nanotoxicity was often accounted for based on dissolved metal content, with little evidence provided for "nano" induced toxicity. Perhaps the bias towards interpreting toxicity effects as a consequence of dissolution could be ascribed to the current limited analytical ability to detect, characterise and quantify ENPs in complex environmental matrices. A further benefit would be the systematic classification of ENPs into categories under which observed effects are either due to solutes, particulates, or both. This will become a reality as the analytical ability to detect, characterise and quantify ENPs in complex environmental matrices improves.

- Overall, based on the literature reviewed, we conclude that the uptake dynamics of ENPs are poorly understood. To date, very few studies have investigated the uptake of ENPs by plants, which is an important factor providing evidence of adsorption or internalisation (Table 1). Rather, many studies used the bioaccumulated metal proportion, which is an indirect indicator that cannot distinguish between adsorbed and internalised ENPs fractions. Bioaccumulation reports showed that aquatic higher plants can serve as reservoirs of ENPs and released soluble metals, and potentially transfer such contaminants between trophic levels in aquatic ecosystems. This is independent of the accumulation pathway (adsorption/uptake). However, the bioaccumulation potential can be manipulated for phytoextraction of nano pollutants in water resources.

- The current data provides a good basis for evaluating the potential risks of ENPs to aquatic higher plants. However, justification exists for additional research aimed at

addressing the gaps identified, in order to undertake risk evaluation under more realistic environmental exposure scenarios.

- The wide range of testing protocols and species makes it difficult to draw meaningful conclusions about toxicity effects such as species sensitivity or endpoint sensitivity. However, in general highly soluble ENPs appear likely to possess elevated toxicity effects, based on rapid uptake of dissolved metal forms. But nano driven toxicity cannot simply be overlooked, as shown by the high oxidative toxicity of nAg compared to soluble Ag. For ENPs known to be photoactive, the influence of exposure light intensity needs to be further studied and considered when interpreting findings. Furthermore, for harmonising future studies, a focus on photosynthetic and growth effects would be useful, because studies in these areas tend to be more cost effective than investigations of subcellular effects, which often require costly reagents. Subcellular studies could then be a component of higher tier testing, following the assessment of growth and photosynthetic effects.

Acknowledgment—M. Thwala acknowledges the UNESCO Keizo Obuchi Fellowship 2014 undertaken at Environmental Toxicology Unit, Clemson University (USA) and the Thuthuka Programme of the National Research Foundation (South Africa). Sponsorship of the present work by the CSIR under the project "Nanotechnology risk assessment in aquatic systems: Experimental and modelling approaches" is also acknowledged. We also thank the editorial contribution provided by M. Silberbauer. The authors declare no conflict of interest.

Data availability—All the information used in this review is cited. Furthermore, Tables 1-5 lists studies which are cited in different sections of the manuscript, therefore such information is publicly available. No additional information is withheld by the authors.

REFERENCES

1. Colvin VL. 2003. The potential environmental impact of nanomaterials. *Nat Biotechnol* 21(10): 1166-1170.

2. Oberdörster E. 2004. Manufactured nanomaterials (fullerenes, C_{60}) induce oxidative stress in the brain of juvenile Largemouth Bass. *Environ Health Perspect* 112(10): 1058-1062.

3. Oberdörster G, Oberdörster E, Oberdörster J. 2005. Nanotoxicology: an emerging discipline evolving from studies of ultrafine particles. *Environ Health Perspect* 113(7): 823-839.

4. Nel A, Xia T, Madler L, Li N. 2006. Toxic potential of materials at the nanolevel. *Science* 311(5761): 622-627.

5. Jolivet J, Froidefond C, Pottier A, Chanéac C, Cassaignon S, Tronc E, Euzen P. 2004. Size tailoring of oxide nanoparticles by precipitation in aqueous medium. A semi-quantitative modelling. *J Mater Chem* 14: 3281-3288.

6. Auffan M, Rose J, Proux O, Borschneck D, Masion A, Chaurand P, Hazemann JL, Chaneac C, Jolivet JP, Wiesner MR, Geen AV, Bottero JY. 2008. Enhanced adsorption of arsenic onto maghemites nanoparticles: As(III) as a probe of the surface structure and heterogeneity. *Langmuir*, 24(7): 3215-3222.

7. BCC Research. 2012. Nanotechnology: a realistic market research, NANO31E, Wellesley, USA.

8. PEN (Project on Emerging Nanotechnologies). 2015. Consumer Products Inventory. Retrieved [02 February 2015], http://www.nanotechproject.org/cpi/about/analysis/

9. Benn TM, Westerhoff P. 2008. Nanoparticle silver released into water from commercially available sock fabrics. *Environ Sci Technol* 42(11): 4133-4139.

10. Kaegi R, Voegelin A, Ort C, Sinnet B, Thalman B, Krismer J, Hagendorfer H, Elumelu M, Mueller E. 2013. Fate and transformation of silver nanoparticles in urban wastewater systems. *Water Res* 47(12): 3866-3877.

11. Kirkegaard P, Hansen SF, Rygaard M. 2015. Potential exposure and treatment efficiency of nanoparticles in water supplies based on wastewater reclamation. *Environ Sci Nano* 2: 191-202.

12. Musee N, Zvimba JN, Schaefer LM, Nota N, Sikhwivhilu LM, Thwala M. 2014. Fate and behavior of ZnO- and Ag-engineered nanoparticles and a bacterial viability assessment in a simulated wastewater treatment plant. *J Environ Sci Health A* 49: 59-66.

13. Hund-Rinke K, Herrchen M, Schlich K. 2014. Integrative test strategy for the environmental assessment of nanomaterials. Federal Environment Agency, Project No. (FKZ) 3712 65 409.

14. Kahru A, Ivask A. 2013. Mapping the dawn of nanoecotoxicological research. *Acc Chem Res* 46(3): 823-833.

15. Donaldson K, Stone V, Tran CL, Kreyling W, Borm PJ.A. 2004. Nanotoxicology. *Occup Environ Med* 61(9): 727-728.

16. Kreyling W, Semmler-Behnke M, Möller W. 2006. Health implications of nanoparticles. *J Nanopar Res* 8 (5): 543-562.

17. Baun A, Hartmann NB, Grieger K, Kusk KO. 2008. Ecotoxicity of nanoparticles to aquatic invertebrates: a brief review and recommendations for future toxicity testing. *Ecotoxicol* 17(5): 387-95.

18. Xia T, Li N, Nel AE. 2009. Potential health impact of nanoparticles. *Annu Rev Public Health* 30 (1): 137-150.

19. Oberdörster E, Zhu SQ, Blickley TM, Clellan-Green P, Haasch ML. 2006. Ecotoxicology of carbon-based engineered nanoparticles: effects of fullerene (C_{60}) on aquatic organisms. *Carbon* 44(6): 1112-1120.

20. Handy RD, Shaw BJ. 2007. Toxic effects of nanoparticles and nanomaterials: implications for public health, risk assessment and the public perception of nanotechnology. *Health Risk Soc* 9(2): 125-144.

21. Moore MN. 2006. Do nanoparticles present ecotoxicological risks for the health of the aquatic environment? *Environ Int* 32(8): 967-976.

22. Kahru A, Dubourguier HC. 2010. From ecotoxicology to nano-ecotoxicology. *Toxicol* 269(2-3): 105-119.

23. Behra R, Krug H. 2008. Nanoecotoxicology-nanoparticles at large. *Nat Nanotechnol* 3(5): 253-254.

24. Handy RD, von der Kammer F, Lead JR, Martin Hassellov M, Richard Owen R, Crane M. 2008. The ecotoxicology and chemistry of manufactured nanoparticles. *Ecotoxicol* 17(4): 287-314.

25. Klaine SJ, Alvarez PJJ, Batley GE, Fernandes TF, Handy RD, Lyon DY, Mahendra S, Mclaughlin MJ, Lead JR. 2008. Nanomaterials in the environment: behaviour, fate, bioavailability, and effects. *Environ Toxicol Chem* 27(9): 1825-1851.

26. Heinlaan M, Ivask A, Blinova I, Dubourguier H, Kahru A. 2008. Toxicity of nanosized and bulk ZnO, CuO and TiO_2 to bacteria *Vibrio fischeri* and crustaceans *Daphnia magna* and *Thamnocephalus platyurus. Chemosphere* 71(7): 1308-1316.

27. Barnes RJ, van der Gast C, Riba O, Lehtovirta LE, Prosse JI, Dobson PJ, Thompson IP. 2010. The impact of zero-valent iron nanoparticles on a river water bacterial community. *J Hazard Mater* 184(1-3): 73-80.

28. Musee N, Thwala M, Nota N. 2011. The antibacterial effects of engineered nanomaterials: implications for wastewater treatment plants. *J Environ Monitor* 13: 1164-1183.

29. von Moos N, Bowen P, Slaveykova VI. 2014. Bioavailability of inorganic nanoparticles to planktonic bacteria and aquatic microalgae in freshwater. *Environ Sci Nano* 1: 214-232.

30. Ji J, Long Z, Lin D. 2011. Toxicity of oxide nanoparticles to the green algae *Chlorella sp. Chem Eng J* 170(2-30: 525-530.

31. Quigg A, Chin W, Chen C, Zhang S, Joang Y, Miao A, Schwer KA, Xu C, Santchi PH. 2013. Direct and indirect toxic effects of engineered nanoparticles on algae: role of natural organic matter. *ACS Sustain Chem Eng* 1(7): 686-702.

32. Lovern SB, Owen HA, Klaper R. 2008. Electron microscopy of gold nanoparticle intake in the gut of *Daphnia magna*. *Nanotoxicol* 2(1):43-48.

33. Li T, Albee B, Alemayehu M, Diaz R, Ingahm L, Kamal S, Rodriguez M and Bishnoi SW. 2010. Comparative toxicity study of Ag, Au, and Ag- Au bimetallic nanoparticles on *Daphnia magna*. *Anal Bioanal Chem* 398(2): 689-700.

34. Lee B, Ranville JF. 2012. The effect of hardness on the stability of citrate-stabilized gold nanoparticles and their uptake by *Daphnia magna*. *J Hazard Mater* 213-214: 434-439.

35. Wray AT, Klaine SJ. 2015. Modeling the influence of physicochemical properties of gold nanoparticle uptake and elimination by *Daphina magna*, *Environ Sci Technol* 34(4): 860-872.

36. Johnston BD, Scown TS, Moder J, Cumberland SA, Baalousha M, Linge K, van Aerle R, Jarvis K, Lead JR, Tyler CR. 2010. Bioavailability of nanoscale metal oxides TiO_2, CeO_2, and ZnO to fish. *Environ Sci Technol* 44(3): 1144-1151.

37. Shaw BJ, Handy RD. 2011. Physiological effects of nanoparticles on fish: a comparison of nanometals versus metal ions. *Environ Int* 37(6): 1083-1097.

38. He X, Aker WG, Hwang H. 2014. An *in vivo* study on the photo-enhanced toxicities of S-doped TiO_2 nanoparticles to zebrafish embryos (*Danio rerio*) in terms of malformation, mortality, rheotaxis dysfuntion, and DNA damage. *Nanotoxicol* 8(1): 185-195.

39. Lahive E, O'Halloran J, Jansen M. 2014. A marriage of convenience; a simple food chain comprised of *Lemna minor* (L.) and *Gammarus pulex* (L.) to study the dietary transfer of zinc. *Plant Biol*, 17(1): 75-81.

40. Peralta-Videa JR, Zhao L, Lopez-Moreno ML, de la Rosa G, Hong J, Gardea-Torresdey JL. 2011 Nanomaterials and the environment: a review for the biennium 2008-2010. *J Hazard Mater* 186 (1): 1-15.

41. Miralles P, Church TL, Harris AT. 2012. Toxicity, uptake, and translocation of engineered nanomaterials in vascular plants. *Environ Sci Technol* 46(17): 9224-9239.

42. Glenn JB, Klaine SJ. 2013. Abiotic and biotic factors that influence the bioavailability of gold nanoparticles to aquatic macrophytes. *Environ Sci Technol* 47(18): 10223-10230.

43. Ma H, Williams PL, Diamond SA. 2013. Ecotoxicity of manufactured ZnO nanoparticles: a review. *Environ Poll* 172: 76-85.

44. Thwala M, Musee N, Sikhwivhilu LM, Wepener V. 2013. The oxidative toxicity of Ag and ZnO nanoparticles towards the aquatic plant *Spirodela punctuta* and the role of testing media parameters. *Environ Sci Process Impact* 15: 1830-1843.

45. Glenn JB, White SA, Klaine SJ. 2012. Interactions of gold nanoparticles with aquatic macrophytes are size and species dependent. *Environ Toxicol Chem* 31(1): 194-201.

46. Holden PA, Nisbet RM, Lenihan HS, Miller RJ, Cherr GN, Schimel JP, Gardea-Torresdey JL. 2013. Ecological nanotoxicology: Integrating nanomaterial hazard considerations across the subcellular, population, community, and ecosystems levels. *Acc Chem Res* 46(3); 813-822.

47. Fairbrother A, Wenstell R, Sappington K, Wood W. 2007. Framework for metals analysis. *Ecotox Environ Safe* 68(2): 145-227.

48. Delay M, Frimmel FH. 2012. Nanoparticles in aquatic systems. *Anal Bioanal Chem* 402(2): 583-592.

49. Unrine JM, Colman BP, Bone AJ, Gondikas AP, Matson CW. 2012. Biotic and abiotic interactions in aquatic microcosms determine fate and toxicity of Ag nanoparticles. Part 1. Aggregation and dissolution. *Environ SciTechnol* 46(13): 6915-6924.

50. Stone V, Nowack B, Baun A, van den Brink N, von der Kammer F, Dusinska M, Handy R, Hankin S, Hassellöv M, Joner E, Fernandes TF. 2010. Nanomaterials for environmental studies: Classification, reference material issues, and strategies for physico-chemical characterisation. *Sci Tot Environ* 408(7): 1745-1754.

51. Nowack B, Ranville JF, Diamond S, Gallego-Urrea JA, Metcalfe C, Rose J, Horne N, Koelmans AA, Klaine SJ. 2012. Potential scenarios for nanomaterials release and subsequent alteration in the environment. *Environ Toxicol Chem* 31(1): 50–59.

52. Auffan M, Rose J, Wiesner MR, Bottero J. 2009. Chemical stability of metallic nanoparticles: A parameter controlling their potential cellular toxicity in vitro. *Environ Poll* 157(4): 1127-1133.

53. Bone AJ, Colman BP, Gondikas AP, Newton KM, Harrold KH, Cory RM, Unrine JM, Klaine SJ, Matson CW, Di Giulio RT. 2012. Biotic and abiotic interactions in aquatic microcosms determine fate and toxicity of Ag nanoparticles: Part 2-toxicity and Ag speciation. *Environ Sci Technol* 46(13): 6925-6933.

54. Jiang H, Li M, Chang F, LI W, Yin L. 2012. Physiological analysis of silver nanoparticles and $AgNO_3$ toxicity to *Spirodela polyrhiza. Environ Toxicol Chem* 31(8): 1880-1886.

55. Hu C, Liu Y, Li X, Li M. 2013. Biochemical responses of duckweed (*Spirodela polyrhiza*) to zinc oxide nanoparticles. *Arch Environ Contam Toxicol* 64: 643-651.

56. Yeo M, Nam D. 2013. Influence of different types of nanomaterials on their bioaccumulation in a paddy microcosm: a comparison of TiO_2 nanoparticles and nanotubes. *Environ Poll* 178: 166-172.

57. Yin L, Cheng Y, Espinasse B, Colman BP, Auffan M, Wiesner M, Rose J, Liu J, Bernhardt ES. 2011. More than the ions: the effects of silver nanoparticles on *Lolium multiflorum*. *Environ Sci Technol* 45(6): 2360-2367.

58. Hu C, Liu X, Li X, Zhao Y. 2014. Evaluation of growth and biochemical indicators of *Salvinia natans* exposed to zinc oxide nanoparticles and zinc accumulation in plants. *Environ Sci Poll Res* 21(1): 732-739.

59. Stebounova LS, Guio E, Grassian VH. 2011. Silver nanoparticles in simulated biological media: a study of aggregation, sedimentation, and dissolution. *J Nanopart Res* 13(1): 233-244.

60. Remedios C, Rosario F, Bastos V. 2012. Environmental nanoparticles interactions with plants: morphological, physiological, and genotoxic aspects. *J Bot* 2012: 1-8.

61. Delay M, Dolt T, Woellhaf A, Sembritzki R, Frimmel FH. 2011. Interactions and stability of silver nanoparticles in the aqueous phase: influence of natural organic matter (NOM) and ionic strength. *J Chromatogr* A 1218(27): 4206-4212.

62. Fabrega J, Luoma SM, Tyler CR, Galloway TS, Lead JR. 2011. Silver nanoparticles: behaviour and effects in the aquatic environment. *Environ Int* 37(2): 517-531.

63. Levard C, Hotze EM, Lowry GV, Brown GE Jr. 2012. Environmental transformations of silver nanoparticles: impact on stability and toxicity. *Environ Sci Technol* 46(13): 6900-6914.

64. Fatehah MO, Aziz HA, Stoll S. 2014. Nanoparticle properties, behaviour, fate in aquatic systems and characterisation methods. *J Coll Sci Biotechnol* 3(2): 1-30.

65. Bian S, Mudumkotuwa IA, Rupasinghe, Grassian VH. 2011. Aggregation and dissolution of 4 nm ZnO nanoparticles in aqueous environments: influence of pH, ionic strength, size, and adsorption of humic acid. *Langmuir* 27(10): 6059-6068.

66. Campbell PGC. 1995. Interactions between trace metals and aquatic organisms: a critique of the free-ion activity model. In Tessier A, Turner DR, eds, *Metal speciation and bioavailability in aquatic systems*. Wiley, Chichester, England, pp 45-102.

67. Reed RB, Ladner DA, Higgins CP, Westerhoff P, Ranville JF. 2012. Solubility of nano-zinc oxide in environmentally and biologically important matrices. *Environ Toxicol Chem* 31(1): 93-99.

68. Turner T, Brice D, Brown MT. 2012. Interactions of silver nanoparticles with the marine macroalga *Ulva lactuta*. *Ecotoxicol* 21(1): 148-154.

69. Chernousova S, Epple M. 2013. Silver as antibacterial agent: ion, nanoparticle, and metal. *Angew Chem Int Edit* 52(6): 1636-653.

70. Luyts K, Napierska D, Nemery B, Hoet PHM. 2013. How physico-chemical characteristics of nanoparticles cause their toxicity: complex and unresolved interrelations. *Environ Sci Proc Imp* 15: 23-38.

71. Odzak N, Kistler D, Behra R, Sigg L. 2014. Dissolution of metal and metal oxide nanoparticles in aqueous media. *Environ Poll* 191: 132-138.

72. Ma X, Geiser-Lee J, Deng Y, Kolmakov A. 2010. Interactions between engineered nanoparticles (ENPs) and plants: phytotoxicity, uptake and accumulation. *Sci Tot Environ* 408(16): 3053-3061.

73. Nair R, Varghese SH, Nair BG, Maekawa T, Yoshida Y, Kumar DS, 2010. Nanoparticulate material delivery to plants. *Plant Sci*. 179(3): 154-163.

74. Li L, Sillanpaa M, Tuominen M, Lounatmaa K, Schultz E. 2013. Behavior of titanium dioxide nanoparticles in *Lemna minor* growth test conditions. *Ecotoxicol Environ Safe* 88: 89-94.

75. Zhang D, Hua T, Xiao F, Chen C, Gersberg RM, Liu Y, Ng WJ, Tan SK. 2014. Uptake and accumulation of CuO nanoparticles and CdS/ZnS quantum dot nanoparticles by *Schoenoplectus tabernaemontani* in hydroponic mesocosms. *Ecol eng* 70: 114-123.

76. Dietz K, Herth S. 2011. Plant nanotoxicology. *Trends Plant Sci* 16(11): 582-589.

77. Sabo-Attwood T, Unrine JM, Stone JW, Murphy CJ, Ghoshroy S, Blom D, Bertsch PM, Newman LA. 2011. Uptake, distribution and toxicity of gold nanoparticles in tobacco (*Nicotiana xanthi*) seedlings. *Nanotoxicol* 6(4): 353-360.

78. Lin D, Xing B. 2008. Root uptake and phytotoxicity of ZnO nanoparticles. *Environ Sci Technol* 42(15): 5580-5585.

79. Carpita N, Sabularse D, Montezinos D, Delmer DP. 1979. Determination of the pore size of cell walls of living plant cells. *Science* 205 (4411): 1144-1147.

80. Adani F, Papa G, Schievano A, Cardinale G, D' Imporzano G, Tambone F. 2011. Nanoscale structure of the cell wall protecting cellulose from enzyme attack. *Environ Sci Technol* 45(3): 1107-1113.

81. Judy JD, Unrine JM, Rao W, W Sue, Bertsch PM. 2012. Bioavailability of gold nanomaterials to plants: importance of particle size and surface coating. *Environ Sci Technol* 46(15): 8467-8474.

82. Rico CM, Majumdar S, Duarte-Gardea M, Peralta-Videa JR, Gardea-Torresdey JL. 2011. Interaction of nanoparticles with edible plants and their possible implications in the food chain. *J Agric Food Chem* 59(8): 3485-3498.

83. Yruela I. 2009. Copper in plants: acquisition, transport and interactions. *Funct Plant Biol* 36(5): 409-430.

84. Festa RA, Thiele DJ. 2011. Copper: an essential metal in biology. *Curr Biol* 21(21): 877-883.

85. Xu Y, Feng L, Jeffrey PD, Shi YG, Morel FM. 2008. Structure and metal exchange in the cadmium carbonic anhydrase of marine diatoms. *Nature* 452(7183): 56-62**.**

86. Etxeberria E. Gonzalez P. Baroja-Fernandez E. Pozueta-Romero J. 2006. Fluid-phase uptake of artificial nano-spheres and fluorescent quantum-dots by sycamore cultured cells. *Plant Signal Behav* 1(4): 181-185.

87. Liu Q, Chen B, Wang Q, Shi X, Xiao Z, Lin J, Fang X. 2009. Carbon nanotubes as molecular transporters for walled plant cells. *Nano Lett* 9 (3): 1007-1010.

88. Smirnova E, Gusev A, Zaytseva O. 2012. Uptake and accumulation of multiwalled carbon nanotubes change the morphometric and biochemical characteristics of *Onobrychis arenaria* seedlings. *Front Chem Sci Eng* 6(2): 132-138,

89. Bian J, Berninger JP, Fulton BA, Brooks BE. 2013. Nutrient stoichiometry and concentrations influence silver toxicity in the aquatic macrophyte *Lemna gibba*. *Sci Tot Environ*, 449: 229-236.

90. Aslani F, Bagheri S, Julkapli NM, Juraimi AS, Hashemi FS, Baghdadi A. 2014. Effects of engineered nanomaterials on plant growth: an overview. *The Sci World J* 449: 1-28.

91. Kurepa J, Paunesku T, Vogt S, Arora H, Rabatic BM, Lu J, Wanzer M B, Woloschak GE, Smalle JA. 2010. Uptake and distribution of ultrasmall anatase TiO_2 Alizarin red S nanoconjugates in *Arabidopsis thaliana*. *Nano Lett* 10(7): 2296-2302.

92. Lee CW, Mahendra S, Zodrow K, Li D, Tsai YC, Braam J, Alvarez PJJ. 2010. Developmental phytotoxicity of metal oxide nanoparticles to *Arabidopsis thaliana*. *Environ Toxicol Chem* 29(3): 669−675.

93. Lin S, Reppert J, Hu Q, Hunson JS, Reid ML, Ratnikova T. 2009. Uptake, translocation and transmission of carbon nanomaterials in rice plants. *Small* 5(10): 1128-1132.

94. Chen R, Ratnikova TA, Stone MB, Lin S, Lard M, Huang G, Hudson JS, Ke PC. 2010. Differential uptake of carbon nanoparticles by plant and mammalian cells. *Small* 6(5): 612-617.

95. Perreault F, Samadani M, Dewez D. 2014. Effect of soluble copper released from copper oxide nanoparticles solubilisation on growth and photosynthetic processes of *Lemna gibba*. *Nanotoxicol* 8(14): 374-382.

96. Dhir B, Sharmila P, Saradhi PP, Nasim SA. 2009. Physiological and antioxidant responses of *Salvinia natans* exposed to chromium-rich wastewater. *Ecotoxicol Environ Saf* 72(6): 1790–1797.

97. Prado C, Rodríguez-Montelongo L, González JA, Pagano EA,Hilal M, Prado FE. 2010. Uptake of chromium by *Salvinia minima*: Effect on plant growth, leaf respiration and carbohydrate metabolism. *J Hazard Mater* 177(1-3): 546–553.

98. Oliver JD. 1993. A review of the biology of giant Salvinia. *J Aqua Plant Manage* 31: 227-231.

99. Smith AR, Pryer KM, Schuettpelz E, Korall P, Schneider H, Wolf PG. 2006. A classification for extant ferns. *Taxonomy* 55(3): 705-731.

100. Perreault F, Popovic R, Dewez D. 2014. Different toxicity mechanisms between bare and polymer-coated copper oxide nanoparticles in *Lemna gibba*. *Environ Poll* 185: 219-227.

101. Perreault F, Oukarroum A, Melegari SP, Matias WG, Popovic, R. 2012. Polymer coating of copper oxide nanoparticles increases nanoparticles uptake and toxicity in the green alga *Chlamydomonas reinhardtii*. *Chemos* 87(11): 1388-1394.

102. Shi J, Abid AD, Kennedy IM, Hristova KR, Silk WK. 2011. To duckweeds (*Landoltia punctata*), nanoparticulate copper oxide is more inhibitory than the soluble copper in the bulk solution. *Environ Poll* 159(5): 1277-1282.

103. Ferry JL, Craig P, Hexel C, Sisco P, Frey R, Pennington PL, Fulton MH, Scott IG, Decho AW, Kashiwada S, Murphy CJ, Shaw T. 2009. Transfer of gold nanoparticles from the water column to the estuarine food web. *Nat Nanotechnol* 4: 441-444.

104. Burns JM, Pennington PL, Sisco PN, Frey R, Kashiwada S, Fulton MH, Scott GI, Decho AW, Murphy CJ, Shaw TJ and Ferry JL. 2013. Surface charge controls the fate of Au nanorods in saline estuaries. *Environ Sci Technol* 47(22): 12844-12851.

105. Griffitt RJ, Luo J, Gao J, Bonzongo J, Barber DS. 2008. Effects of particle composition and species on toxicity of metallic nanomaterials in aquatic organisms. *Environ Toxicol Chem* 27(9): 1972-1978.

106. Liu J, Wang Z, Liu FD, Kane AB, Hurt BH. 2012. Chemical transformations of nanosilver in biological environments. *ACS Nano* 6(11): 9887-9899.

107. Oukarroum A, Barhoumi L, Pirastru L, Dewez D. 2013. Silver nanoparticle toxicity effects on growth and cellular viability of the aquatic plant *Lemna gibba*. *Environ Toxicol Chem* 32(4): 902–907.

108. Jiang H, Qiu X, Li G, Li W, Yin L. 2014. Silver nanoparticles induced accumulation of reactive oxygen species and alteration of antioxidant systems in the aquatic plant *Spirodela polyrhiza*. *Environ Toxicol Chem* 33(6): 1398-1405.

109. McGeer JM, Brix KV, Skeaff JM, DeForest DK, Brigham SI, Adams WJ, Green A. 2003. Inverse relationship between bioconcentration factor and exposure concentration for metals: implications for hazard assessment of metals in the aquatic environment. *Environ Toxicol Chem* 22(5): 1017-1037.

110. Song G, Gao Y, Wu H, Hou W, Zhang C, Ma H. 2012 . Physiological effect of anatase TiO_2 nanoparticles on *Lemna minor*. *Environ Toxicol Chem* 31(9): 2147–2152.

111. Maksymiec W. 1997. Effect of copper on cellular processes in higher plants. *Photosynthetica* 34(3): 321-342.

112. Juhel G, Batisse E, Hugues Q, Daly D, van Pelt F, O'Halloran J, Jansen MAK. 2011. Alumina nanoparticles enhance growth of *Lemna minor*. *Aqua Toxicol* 105(3-4): 328-336.

113. Gubbins EJ, Batty LC, Lead JR. 2011. Phytotoxicity of silver nanoparticles to *Lemna minor* L. *Environ Poll* 159(6): 1551-1559.

114. Ucuncu E, Ozkan AD, Kursungoz C, Ulger ZE, Olmez TT, Tekinay T, Ortac B, Tunca E. 2014. Effects of laser ablated silver nanoparticles on *Lemnar minor*. *Chemosphere* 108: 251-257.

115. Kim E, Kim S, Kim H, Lee SG, Lee SJ, Jeong SW. 2011. Growth inhibition of aquatic plant caused by silver and titanium oxide nanoparticles. *Toxicol Environ Health Sci* 3(1): 1-6.

Figure 1. Schematic presentation of transformations that metal-based ENPs undergo in aqueous environments. These are amongst key processes that determine behaviour (chemical and physical) and bioavailability of metal-based ENPs in aquatic ecosystems.

Table 1: Summary of metal-based ENPs accumulation pathways by aquatic higher plants.

Uptake pathway	ENP type	Uptake detection method	ENPs characteristics	Exposure water	Plant	Reference
Internalisation (tissue)	nAu	TEM; STEM and SEM; and EDX	4 nm; spherical; ζ -14.1 mV; 250 g/L	Well/borehole water; pH 7.1; TOC 8.56 mg/L; $CaCO_3$ 107 mg/L; conductivity 210 µS/cm	*Myriophyllum simulans*	[45]
Internalisation (cellular)	nAu	TEM; STEM and SEM; and EDX	4 nm; 18 nm; spherical; ζ -14.1 mV; ζ -9.73 mV	Well/borehole water; pH 7.1; TOC 8.56 mg/L; $CaCO_3$ 107 mg/L; conductivity 210 µS/cm	*Azolla caroliniana*	[45]
Adsorption (no internalisation)	nAu	TEM; STEM and SEM; and EDX	4 nm; 18 nm; spherical; ζ -14.1 mV; ζ -9.73 mV	Well/borehole water; pH 7.1; TOC 8.56 mg/L; $CaCO_3$ 107 mg/L; conductivity 210 µS/cm	*Egeria densa*	[45]
Adsorption (no internalisation)	$nTiO_2$	SEM; TEM	275–2398 nm; SSA 50 m^2/g; 0.01–10 mg/L	Steinburg growth medium; pH 5.5; $CaCO_3$ 166 mg/L	*Lemna minor*	[74]
Adsorption (roots)	CdS QDs	TEM	4.3 nm; ζ -9.8 mV	Hoagland's medium	*Schoenoplectus tabernaemontani*	[75]
Adsorption (roots)	nCuO	TEM	38 nm; SSA 12.84 m^2/g; ζ -2.8 mV	Hoagland's medium	*S. tabernaemontani*	[75]
Tissue and cellular internalisation	CdS QDs	TEM	4.3 nm; ζ -9.8 mV	Hoagland's medium	*S. tabernaemontani*	[75]
Tissue and cellular internalisation	nCuO	TEM	38±7 nm; SSA 12.84 m^2/g; ζ -2.8 mV	Hoagland's medium	*S. tabernaemontani*	[75]
Adsorption	nZnO	ICP-OES	25 nm; uncoated; SSA 90 m^2/g; 1–10 mg/L	OECD growth medium; pH 6.5	*Salvinia natans*	[58]

TEM=transmission electron microscopy; STEM=scanning transmission electron microscopy; SEM=scanning electron microscopy; EDX=energy dispersive x-ray spectroscopy; TOC=total organic carbon; SSA=specific surface area; ICP-OES=inductively coupled plasma optical emission spectrometry; OECD=Organisation for Economic Co-operation and Development; ζ=zeta potential

Table 2: Summary findings on the bioaccumulation of ENPs by aquatic higher plants.

ENPs	ENPs characteristics	Exposure concentration	Exposure water	Exposure duration	Bioaccumulation	Plant	Reference
nZnO	25 nm; SSA 90 m^2/g	1–50 mg/L	Hoagland's medium; pH 6.5	96 hours	2–4.5 mg/g (whole plants) estimated (est).	*Spirdoela polyrhiza*	[55]
nZnO	25 nm; SSA 90 m^2/g	1–50 mg/L	Hoagland's medium; pH 6.5	7 days	0.45–3.65 mg/g (leaves) 0.33–2.97 mg/g (roots rinsed) 0.49–8.18 mg/g (roots unrinsed)	*Salvinia natans*	[58]
$nTiO_2$	275–2398 nm; SSA 50 m^2/g; ζ -20 to -25 mV (est.)	0.01–10 mg/L	Steinburg growth medium; pH 5.5; $CaCO_3$ 166 mg/L	7 days	1–70 mg/kg (whole plant) (est.)	*Lemna minor*	[74]
$nTiO_2$	5–10 nm; rhombic and spherical; ζ -33.83 mV	1.8 mg/L	Mesocosm	17 days	424.4 µg/g (root); 64.7 µg/g (stem)	*Oenanthe javanica*	[56]
					54.5 µg/g (whole plant)	*Isoetes japonia*	[56]
$nTiO_2$ (nanotube)	7–9 nm (width); 2 nm (thick); 6 nm (diameter); tubular; ζ -41.5 mV	1.8 mg/L	Freshwater mesocosm	17 days	73.6 µg/g (root) 5.9 µg/g (stem)	*O. javanica*	[56]
					155.2 µg/g (whole plant)	*I. japonica*	[56]
nCuO	10–15 nm (TEM); 43 nm (SMPS); 6.7 nm (BET); 9 (7 days) ζ -80 nm; SSA 141 m^2/g	1 mg/L	Hoagland's medium; pH 6		800 µg/g (roots) (est.) 700 µg/g (fronds) (est.)	*Landoltia punctata*	[102]
nCuO	318 nm	0.68–4.51 g/L	Freshwater culture medium; pH 6.5; IS 12.7 mM	48 hours	0.001–0.1 mg/mg (whole plant) (est.)	*Lemna gibba*	[95]
nCuO	97 nm; Poly(styrene-co-butyl acrylate) coating; ζ -40 mV	0..25–1.24 g/L	Freshwater culture medium; pH 6.5; IS 12.7 mM	48 hours	0.005–0.025 mg/mg (whole plant) (est.)	*L. gibba*	[100]
nCuO	523 nm; ζ -40 mV	0.68–4.51 g/L	Freshwater culture medium; pH 6.5; IS 12.7 mM	48 hours	0.006–0.01 mg/mg (whole plant) (est.)	*L. gibba*	[100]
nCuO	38 nm; SSA 12.84 m^2/g; ζ -2.8 mV	0.5–50 mg/L	Hoagland's medium	21 days	14–4057 µg/g (roots) 0.8–17.7 µg/g (shoots)	*Schoenoplectus tabernaemontani*	[75]
CdS	4.3 nm; ζ -9.8 mV	0.5–50 mg/L	Hoagland's medium	21 days	9–1518 µg/g (roots) 0.8–8.7 µg/g (shoots)	*S. tabernaemontani*	[75]
nAu	65 x 15 nm; rods	7.08 x 10^8 particles/mL	Estuarine mesocosm; pH 7.7–8.5 (est.); salinity 16.5-18 g/L; DO 5–12 mg/L (est.)	12 days	3.45 µg/kg (whole plant)	*Spartina alterniflora*	[103]
nAu	48.3 x 9.8 nm; rods; ζ -53.5 mV	3.42 x 10^7 particles/mL	Estuarine mesocosm; salinity 20 g/L; pH 8 (est.)	11 days	117 (roots); 4.42 (stems); 1.17 µg/kg (shoots)	*S. alterniflora*	[104]
nAu (4; 18 nm)	4 nm; 18 nm; spherical; -14.1 mV; ζ -9.73 mV	250 µg/L	Well/borehole water; pH 7.1; DOC 8.56 mg/L; $CaCO_3$ 107 mg/L; conductivity 210 µS/cm	24 hours	100 mg/kg (est.); <60 mg/kg (whole plant) (est.)	*Myriophyllum simulans*	[45]
nAu (4; 18	4 nm; 18 nm;	250 µg/L	Well/borehole water; pH 7.1;	24 hours	120 mg/kg (est.); <60 mg/kg (whole plant)	*Azolla caroliniana*	[45]

nm)	spherical; ζ -14.1 mV; ζ -9.73 mV		TOC 8.56 mg/L; $CaCO_3$ 107 mg/L; conductivity 210 µS/cm		(est.)		
nAu (4; 18 nm)	4 nm; 18 nm; spherical; -14.1 mV; -9.73 mV	250 µg/L	Well/borehole water; pH 7.1; TOC 8.56 mg/L; $CaCO_3$ 107 mg/L; conductivity 210 µs/cm	24 hours	40 mg/kg (est.); <60 mg/kg (whole plant) (est.)	*Egeria densa*	[45]
nAu (4; 18; 30 nm)	8 nm; 17.5 nm; 25 nm; ζ -16.7 mV; ζ -17.8 mV; ζ -23.7 mV	250 µg/L	Well/borehole water; pH 6.8; DOC 0.1 mg/L	24 hours	50-150 mg/kg (whole plant) (est.); <50 mg/kg (shoots)	*A. caroliniana*	[42]
nAu (4; 18; 30 nm)	8 nm; 17.5 nm; 25 nm; ζ -16.7 mV; ζ -17.8 mV; ζ -23.7 mV	250 µg/L	Well/borehole water+DOC; pH 6.8; DOC 2±0.4 mg/L	24 hours	<50 mg/kg (whole plant: 4 nm); 50 mg/kg (whole plant: 18; 30 nm)(est.); <50 mg/kg (shoots)	*A. caroliniana*	[42]
nAu (4; 18; 30 nm)	8 nm; 17.5 nm; 25±7 nm; ζ -16.7 mV; ζ -17.8 mV; ζ -23.7 mV	250 µg/L	Well/borehole water; pH 6.8; DOC 0.1 mg/L	24 hours	<50 mg/kg (whole plant); <50 mg/kg (shoots)	*E. densa*	[42]
nAu (4; 18; 30 nm)	8 nm; 17.5 nm; 25 nm; ζ -16.7 mV; ζ -17.8 mV; ζ -23.7 mV	250 µg/L	Well/borehole water+DOC; pH 6.8; DOC 2±0.4 mg/L	24 hours	<50 mg/kg (whole plant); <50 mg/kg (shoots)	*E. densa*	[42]
nAu (4; 18; 30 nm)	8 nm; 17.5 nm; 25 nm; ζ -16.7 mV; ζ -17.8 mV; ζ -23.7 mV	250 µg/L	Well/borehole water; pH 6.8; DOC 0.1 mg/L	24 hours	<50 mg/kg (whole plant); <50 mg/kg (shoots)	*M. simulans*	[42]
nAu (4; 18; 30 nm)	8 nm; 17.5 nm; 25 nm; ζ -16.7 mV; ζ -17.8 mV; ζ -23.7 mV	250 µg/L	Well/borehole water+DOC; pH 6.8; DOC 2 mg/L	24 hours	<50 mg/kg (whole plant); <50 mg/kg (shoots)	*M. simulans*	[42]
nAg	7.8 nm; gum-arabic coating; SSA 100 m^2/g; ζ -49 to -44 mV	0.5-10 mg/L	10% Hoagland's medium	72 hours	2.81 mg/g (whole plant)	*S. polyrhiza*	[54]
nAg	240 nm; spherical; SSA 5-10 m^2/g; ζ -31.49 mV	0.01-10 mg/L	Inorganic growth culture medium; pH 6.5; IS 4.25 mM	7 days	7.72–17.75 µg/mg (whole plant)	*L. gibba*	[107]

SSA=specific surface area; TEM=transmission electron microscopy; SMPS=scanning mobility particle sizer; BET=Brunauer–Emmett–Teller method; IS=ionic strength; DOC=dissolved organic carbon; ζ=zeta potential

Table 3: Summary of subcellular effects in aquatic higher plants exposed to metal-based ENPs.

ENPs	ENPs characteristics	Exposure water	Exposure concentration	Duration	Endpoint	Effect/response	Plant	Reference
nCuO	523 nm; ζ -40 mV	Freshwater culture medium; pH 6.5; IS 12.7 mM	0.7–4.5 g/L	48 hours	Esterase ROS	Decreased Increased	*Lemna gibba*	[100]
nCuO	97 nm; Poly(styrene-co-butyl acrylate) coating; ζ -40 mV	Freshwater culture medium; pH 6.5; IS 12.7 mM	0.3–1.2 g/L	48 hours	Esterase ROS	Decreased Increased	*L. gibba*	[100]
$nTiO_2$	10 nm; ζ -15 to 25 mV(est.); SSA 120 m^2/g	10% Steinberg medium; irradiance 72 µmol/m^2/s	10–2000 mg/L	7 days	POD CAT SOD MDA	Activated Activated Activated then inhibited Increased	*Lemna minor*	[110]
nZnO	25 nm; uncoated; 90 m^2/g; spherical	Hoagland's medium; pH 6.5	1–50 mg/L	96 hours	CAT POD SOD Na^+K^+ATPase	Activated (50 mg/L) Inhibited (50 mg/L) Activated (≥10 mg/L) Uniform	*Spirodela polyrhiza*	[55]
nZnO	25 nm; uncoated; 90 m^2/g; 1–10 mg/L	OECD growth medium; pH 6.5	1–50 mg/L	7 days	SOD CAT POD	Activated (50 mg/L) Activated (50 mg/L) Inhibited (50 mg/L)	*Salvinia natans*	[58]
nAg	240 nm; spherical; SSA 5–10 m^2/g; ζ -31.49±2.16 mV	Inorganic growth culture medium; pH 6.5; IS 4.25 mM	0.01–10 mg/L	7 days	Cell viability ROS formation	Reduced from 0.1 mg/L Increased from 1 mg/L	*L. gibba*	[107]
nZnO	326–1350 nm; ζ -4.9 to 11 mV; SSA 11.4 m^2/g; spheres; polydispersed morphology	Hoagland's medium	0.01–1000 mg/L	14 days	ROS/RNS H_2O_2 TAC SOD	Increased then stabilised (4 days) Increased (14 days) Uniform (4 days) then increased at highest exposure dose (14 days) Increased at lowest exposure dose (4 days) Inhibited (14 days); only activated at highest dosage (14 days)	*Spirodela punctuta*	[44]
nAg	352–1313 nm; ζ -3.6 to 11.6 mV; SSA 3.4 m^2/g; polydispersed morphology	Hoagland's medium	0.01–1000 mg/L	14 days	ROS/RNS H_2O_2 TAC SOD	Uniform (4-14 days) Increased Uniform Inhibited and activated (4 days); inhibited (14 days)	*S. punctuta*	[44]
nAg	7.8 nm; gum-arabic coating; SSA 100 m^2/g; ζ -49 to -44 mV	10% Hoagland's medium	0.5–10 mg/L	72 hours	Nitrate-nitrogen Phosphate-phosphorus Carbohydrate Proline	Reduced (≥5 mg/L) Uniform Uniform (5 mg/L) Increased (≥5m g/L)	*S. polyrhiza*	[54]
nAg	7.8 nm; gum-arabic coating; SSA 100 m^2/g; ζ -49 to -44 mV; spherical	10% Hoagland's medium	0.5–10 mg/L	72 hours	ROS content SOD POD CAT	Increased (≥1 mg/L) Activated Activated (≥5 mg/L) Activated (5 mg/L)	*S. polyrhiza*	[108]

					Protein content MDA GSH	Increased (1;5 mg/L) Increased (5 mg/L) Increased (≥1 mg/L)		
nAg	22.9 nm; PVP coating; spherical	10% Hoagland's medium	10 mg/L	72 hours	ROS content SOD POD CAT Protein content MDA GSH	Increase of ROS; SOD; POD; GSH and protein content. No significant effect on CAT and MDA	*S. polyrhiza*	[108]

IS=ionic strength; ROS=reactive oxygen species; SSA=specific surface area; POD=peroxidase; CAT=catalase; SOD=superoxide dismutase; MDA=malondialdehyde; OECD=Organisation for Economic Co-operation and Development; GSH=glutathione; RNS=reactive nitrogen species; TAC=total antioxidative capacity; PVP=polyvinylpyrrolidone; ζ=zeta potential

Table 4: Summary findings of photosynthetic effects in aquatic higher plants exposed to metal-based ENPs.

ENPs	ENPs characteristics	Exposure water	Exposure concentration	Duration	Endpoint	Effect/response	Plant	Reference
nCuO	109–523 nm	Freshwater culture medium; pH 6.5; IS 12.7 mM	0.68–4.5 g/L	48 hours	PSII activity PSII yield	Decreased Decreased	*L. gibba*	[95]
nCuO	523 nm; ζ -40 mV	Freshwater culture medium; pH 6.5; IS 12.7 mM	0.7–4.5 g/L	48 hours	PSII performance index	Inhibited	*L. gibba*	[100]
nCuO	97 nm; Poly(styrene-co-butyl acrylate) coating; ζ -40 mV	Freshwater culture medium; pH 6.5; IS 12.7 mM	0.3–1.2 g/L	48 hours	PSII performance index	Inhibited	*L. gibba*	[100]
nCuO	10–15 nm (TEM); 43 nm (SMPS); 6.7 nm (BET); 9 (7 days)- 80 nm; SSA 141 m^2/g	Hoagland's medium; pH 6	1 mg/L	14 days	Chl *a* Chl *b* Chl *a*+Chl *b*	Decreased Decreased Decreased	*L. punctata*	[102]
$nTiO_2$	10 nm; ζ -15 to -25 mV (est.)	10% Steinberg medium; pH 6.5; irradiance 72 $\mu mol/m^2/s$	10–2000 mg/L	7 days	Chlorophyll content	Increased (≤200 mg/L)	*L. minor*	[110]
$nTiO_2$	275 –2398 nm; SSA 50 m^2/g	Steinburg growth medium; pH 5.5; $CaCO_3$ 166 mg/L; irradiance 5000 lx	0.01–10 mg/L	7 days	Chl *a*	No significant effects	*L. minor*	[74]
nAl_2O_3	9.01 nm (TEM); 165–189 nm (NTA); SSA 200 m^2/g; spherical to void; ζ 5.3 mV	50% Hutner's medium; pH 5.3	10–1000 mg/L	7 days	PSII yield Photochemical quench Non-photo quench	Increased (100 mg/L) Increased (100 mg/L) No significant effects	*L. minor*	[112]
nZnO	25 nm; SSA 90 m^2/g	Hoagland's medium; pH 6.5	1–50 mg/L	96 hours	Chl:pheophytin	Reduced (50 mg/L)	*S. polyrhiza*	[55]
nZnO	25 nm; SSA 90 m^2/g	Hoagland's medium; pH 6.5	1–50 mg/L	7 days	Chl *a* Chl *b* Carotenoid	Increased (50 mg/L) No effects Increased (50 mg/L)	*S. natans*	[58]
nAg	7.8 nm; gum-arabic coating; SSA 100 m^2/g; ζ -49 to -44 mV	10% Hoagland's medium	0.5–10 mg/L	72 hours	Chl *a* Chl *a/b* Chl total Photochemical efficiency	Decreased Decreased (≥5 mg/L) Decreased Decreased	*S. polyrhiza*	[54]

PSII=photosynthetic system II; TEM=transmission electron microscopy; SMPS=scanning mobility particle sizer; BET=Brunauer–Emmett–Teller method; SSA= specific surface area; NTA=nanoparticle tracking analysis; ζ=zeta potential

Table 5: Summary findings on growth effects in aquatic higher plants exposed to metal-based ENPs.

ENPs	ENPs characteristics	Exposure water	Exposure concentration	Duration	Endpoint	Effect/response	Plant	Reference
nCuO	38 nm; SSA 12.84 m^2/g; ζ -2.8 mV	25% Hoagland's medium	0.5–50 mg/L	21 days	Biomass	No significant effects	*S. tabernaemontani*	[75]
nCdS QDs	4.3 nm; -9.8 mV	25% Hoagland's medium	0.5–50 mg/L	21 days	Biomass	Reduction ≥5 mg/L	*S. tabernaemontani*	[75]
nCuO	109–523 nm	Freshwater culture medium; pH 6.5; IS 12.7 M	0.4–4.5 g/L	48 hours	Growth rate	Growth reduction >0.1 Cu g/L	*L. gibba*	[95]
nCuO	97 nm; Poly(styrene-co-butyl acrylate) coating; ζ -40 mV	Freshwater culture medium; pH 6.5; IS 12.7 M	0.3–1.2 g/L	48 hours	Growth rate	Inhibited	*L. gibba*	[100]
nCuO	523 nm; ζ -40 mV	Freshwater culture medium; pH 6.5; IS 12.7 M	0.7–4.5 g/L	48 hours	Growth rate	Inhibited	*L. gibba*	[100]
nCuO	10–15 nm (TEM); 43 nm (SMPS); 6.7 nm (BET); 9 (7 days) 80 nm; SSA 141 m^2/g	Hoagland's medium; pH 6.5±0.2	0.0158–4 mg/L	96 hours	Frond number	Reduced	*Landoltia punctata*	[102]
			1 mg/L	9 days	Frond number	Reduced	*L. punctata*	[102]
			1 mg/L	9 days	Frond doublings	Reduced	*L. punctata*	[102]
nAg	93.52 nm (TEM); citrate coating; ζ -7.87 mV	OECD 221 medium; pH 5.5	5–160 µg/L	14 days	Frond number	Decreased (≥20 µg/L)	*L. minor*	[113]
					Growth rate	Decreased (≥10 µg/L)		
					Dry weight	Decreased (≥10 µg/L)		
					Growth inhibition	Increased		
nAg	29.2 nm (TEM); citrate coating; ζ -7.87 mV	OECD 221 medium; pH 5.5	5–160 µg/L	14 days	Frond number	Decreased (≥80 µg/L)	*L. minor*	[113]
					Growth rate	Decreased (≥20 µg/L)		
					Dry weight	Decreased (≥20 µg/L)		
					Growth inhibition	Increased		
nAg	7.8 nm; gum-arabic coating; SSA 100 m^2/g; -49 to -44 mV	10% Hoagland's medium	0.5–10 mg/L	72 hours	Fresh weight	Decreased (≥5 µg/L)	*S. polyrhiza*	[54]
					Dry weight	Decreased (≥5 µg/L)		
nAg	240 nm; spherical; SSA 5–10 m^2/g; ζ -31.49 mV	Inorganic growth culture medium; pH 6.5; IS 4.25 mM	0.01–10 mg/L	7 days	Frond number	Reduced	*L. gibba*	[107]
					Growth	Reduced		

nAg	5–20 nm (TEM); 84.97 nm (DLS); spherical; ζ -34.9 mV	Greenhouse water	8–128 µg/L	7 days	Frond number Growth rate Total weight Total fronds Growth inhibition	Decreased Decreased Decreased Decreased Increased	*L. minor*	[114]
nAg	50 nm	Algal assay procedure medium; pH 7.5	0.1–200 mg/L	7 days	Growth rate	Decreased (≥1 mg/L)	*L. pausicostata*	[115]
$nTiO_2$	2-3 nm	Algal assay procedure medium; pH 7.5; irradiance 6500–10000 lx	31.25–500 mg/L	7 days	Growth rate	Decreased (≥250 mg/L)	*L. pausicostata*	[115]
$nTiO_2$	275 - 2398 nm; SSA 50 m^2/g; ζ -25 to -20 mV (est.)	Steinburg growth medium; pH 5.5; $CaCO_3$ 166 mg/L; irradiance 5000 lx	0.01–10 mg/L	*7 days*	Frond number Growth rate	No effects No effects	*L. minor*	[74]
nZnO	25 nm; SSA 90 m^2/g	Hoagland's medium; pH 6.5	1–50 mg/L	7 days	Growth rate Frond number Relative frond number	All inhibited at 50 mg/L	*S. natans*	[55]
nZnO	25 nm; SSA 90 m^2/g	OECD Medium; pH 6.5	1-50 mg/L	7 days	Growth rate	No effects	*S. natans*	[58]
nAl_2O_3	9.01nm (TEM); 165–189 nm (NTA); SSA 200 m^2/g; spherical to void; ζ 5.3 mV	50% Hutner's medium; pH 5.3	10-1000 mg/L	7 days	Biomass	Stimulated	*L. minor*	[112]

SSA=specific surface area; TEM=transmission electron microscopy; SMPS=scanning mobility particle sizer; BET=Brunauer–Emmett–Teller method; IS=ionic strength; OECD=Organisation for Economic Co-operation and Development; DLS=dynamic light scattering; SSA=specific surface area; NTA=nanoparticle tracking analysis; ζ=zeta potential

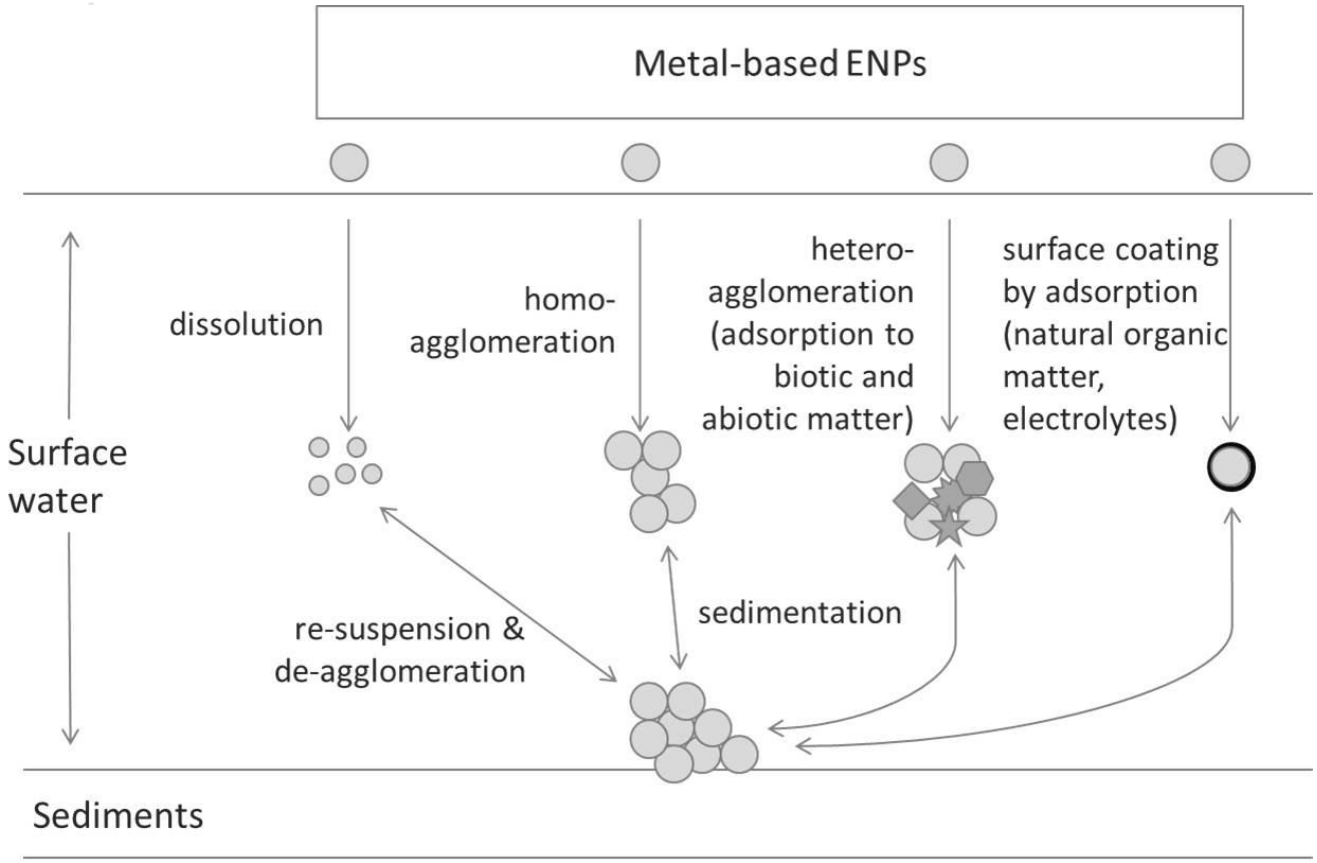

Figure 1